Int J Earth Sci (Geol Rundsch)
DOI 10.1007/s00531-007-0202-2

ORIGINAL PAPER

Separation of rifting and lithospheric folding signatures in the NW-Alpine foreland

O. Bourgeois · M. Ford · M. Diraison · C. Le Carlier de Veslud · M. Gerbault · R. Pik · N. Ruby · S. Bonnet

Received: 28 November 2005 / Accepted: 10 May 2007

Abstract The development of the Alpine mountain belt has been governed by the convergence of the African and European plates since the Late Cretaceous. During the Cenozoic, this orogeny was accompanied with two major kinds of intraplate deformation in the NW-European foreland: (1) the European Cenozoic Rift System (ECRIS), a left-lateral transtensional wrench zone striking NNE-SSW between the western Mediterranean Sea and the Bohemian Massif; (2) long-wavelength lithospheric folds striking NE and located between the Alpine front and the North Sea. The present-day geometry of the European crust comprises the signatures of these two events superimposed on all preceding ones. In order to better define the processes and causes of each event, we identify and separate their respective geometrical signatures on depth maps of the pre-Mesozoic basement and of the Moho. We derive the respective timing of rifting and folding from sedimentary accumulation curves computed for selected locations of the Upper Rhine Graben. From this geometrical and chronological separation, we infer that the ECRIS developed mostly from 37 to 17 Ma, in response to north-directed impingement of Adria into the European plate. Lithospheric folds developed between 17 and 0 Ma, after the azimuth of relative displacement between Adria and Europe turned counter-clockwise to NW–SE. The geometry of these folds (wavelength = 270 km; amplitude = 1,500 m) is consistent with the geometry, as predicted by analogue and numerical models, of buckle folds produced by horizontal shortening of the whole lithosphere. The development of the folds resulted in *ca.* 1,000 m of rock uplift along the hinge lines of the anticlines (Burgundy–Swabian Jura and Normandy–Vogelsberg) and *ca.* 500 m of rock subsidence along the hinge line of the intervening syncline (Sologne–Franconian Basin). The grabens of the ECRIS were tilted by the development of the folds, and their rift-related sedimentary infill was reduced on anticlines, while sedimentary accumulation was enhanced in synclines. We interpret the occurrence of Miocene volcanic activity and of topographic highs, and the basement and Moho configurations in the Vosges–Black Forest area and in the Rhenish Massif as interference patterns between linear lithospheric anticlines and linear grabens, rather than as signatures of asthenospheric plumes.

Keywords Europe · Alps · Cenozoic · Rifting · Folding · Buckling · Moho · Basement · Lithosphere · Crust

O. Bourgeois (✉)
Laboratoire de Planétologie et de Géodynamique,
UMR CNRS 6112, Université de Nantes,
BP 92205, 2 rue de la Houssinière,
44322 Nantes Cedex, France
e-mail: olivier.bourgeois@univ-nantes.fr

M. Ford · C. Le Carlier de Veslud · R. Pik · N. Ruby · S. Bonnet
Centre de Recherches Pétrographiques et Géochimiques,
UPR CNRS 2300, 15 rue Notre Dame des Pauvres,
54501 Vandoeuvre les Nancy, France

M. Diraison
Institut de Physique du Globe de Strasbourg,
UMR CNRS 7516, Centre de Géochimie de la Surface,
UMR CNRS 7517, 1 rue Blessig,
67084 Strasbourg Cedex, France

M. Gerbault
Institut de Recherche pour le Développement,
Dpto geologia, Universitad de Chile, Plaza Ercilla #803,
Casilla 13518 correo 21, Santiago, Chili

Introduction

Two geodynamic events affected the West-European plate during the Cenozoic: (1) the Alpine orogeny, which is related to convergence between the Adriatic and European plates, and which started during the Late Cretaceous and is still ongoing (Dewey et al. 1989; Rosenbaum et al. 2002); (2) the opening of the European Cenozoic Rift System (ECRIS) that started during the Late Eocene. The question of whether and how the Alpine orogeny and the opening of the ECRIS are related to each other are still debated (e.g. Ziegler 1994; Merle and Michon 2001; Michon and Merle 2001, 2005; Dèzes et al. 2004, 2005; Ziegler and Dèzes 2005). However, these events were responsible for two superimposed, partly coeval modes of deformation in the European plate.

The opening of the ECRIS produced lithospheric thinning in a number of grabens located between the Mediterranean Sea to the South-West, the North Sea to the North-West and the Bohemian Massif to the East (Fig. 1). Although the ECRIS has been studied for several decades, its origin is controversial because the timing, the orientation and the magnitude of tectonic motions during its formation are still debated. A variety of hypotheses for its origin have been proposed, involving processes such as plume-related active rifting (Neugebauer 1978), foreland splitting in response to the Alpine orogeny (Sengör 1976; Tapponnier 1977; Sengör et al. 1978; Bergerat and Geyssant 1980; Dewey and Windley 1988; Regenauer-Lieb and Petit 1997; Dèzes et al. 2004, 2005; Ziegler and Dèzes 2005), back-arc rifting (Jowett 1991) or slab-pull (Stampfli et al. 1998;

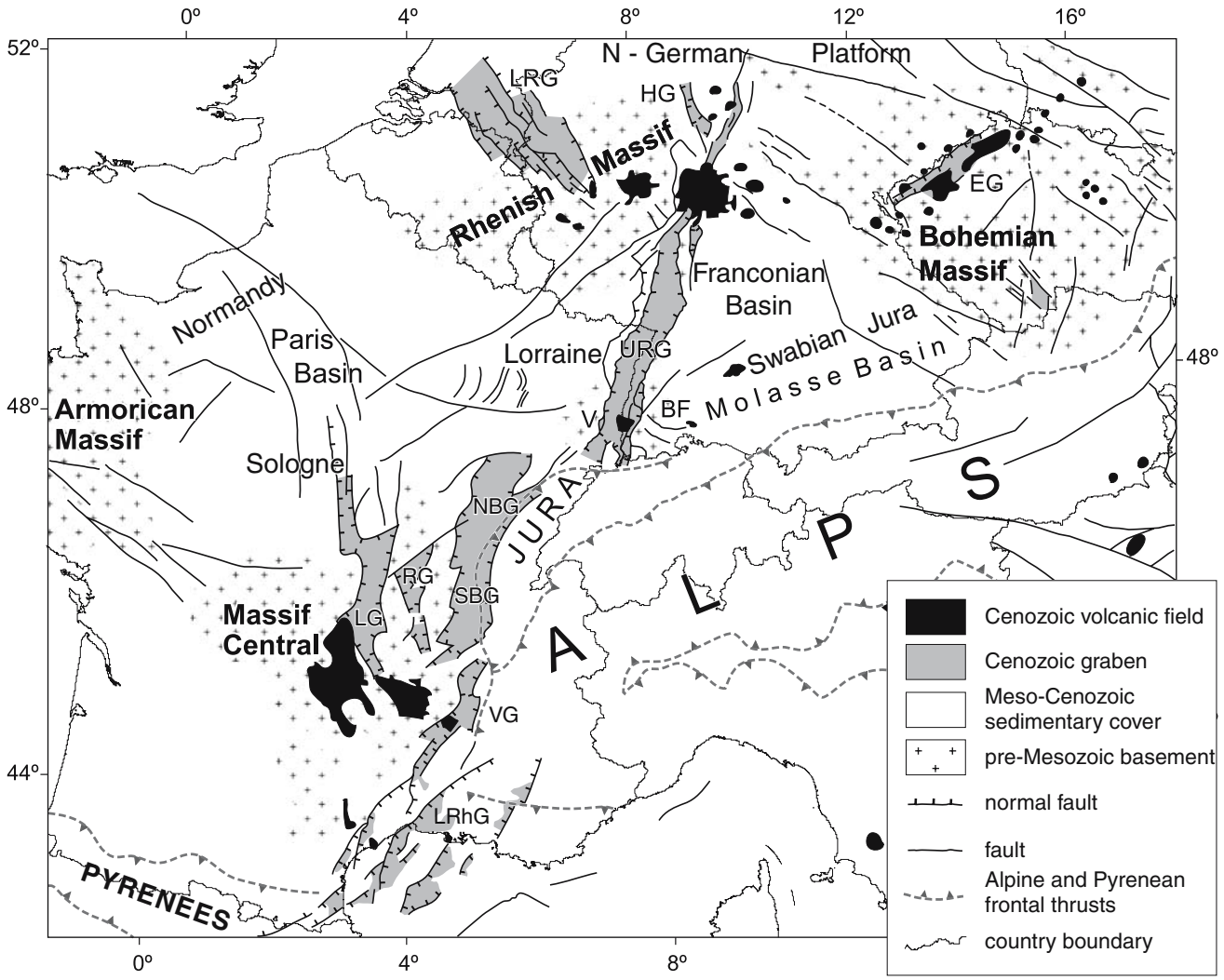

Fig. 1 Structural map of the ECRIS in the NW-Alpine foreland (after Dèzes et al. 2004, modified). *BF* Black Forest, *EG* Eger (Ore) Graben, *FP* Franconian Platform, *HG* Hessian grabens, *LG* Limagne Graben, *LRG* Lower Rhine (Roer Valley) Graben, *LRhG* Lower Rhône Grabens, *NBG* Northern Bresse Graben, *RG* Roanne Graben, *SBG* Southern Bresse Graben, *URG* Upper Rhine Graben, *V* Vosges, *VG* Valence Graben

Merle and Michon 2001; Michon et al. 2003; Michon and Merle 2005). These various interpretations require different magnitudes, orientations and timing for tectonic motions in the ECRIS.

While the Alpine orogeny produced crustal thickening in the Alps, in the Pyrenees and in the Corsica–Betics–Rif mountain belts, it also entailed long-wavelength lithospheric folding of the European foreland. The location, geometry, timing and mechanism of folding are poorly known however. Amongst the currently proposed processes are foreland flexural bending (Gutscher 1995; Burkhard and Sommaruga 1998; Bourgeois et al. 2001; Leseur et al. 2005), far-field intraplate buckling (Lefort and Agarwal 1996, 2002; Guillocheau et al. 2000; Michon and Merle 2001, 2005; Michon et al. 2003; Bourgeois et al. 2004; Dèzes et al. 2004, 2005; Ziegler and Dèzes 2005) or dynamic support by asthenospheric flow (Merle and Michon 2001). Thermal erosion of the lithosphere by up-welling asthenospheric thermal anomalies may also have played a role in the long-wavelength deformation of the European lithosphere (Dèzes et al. 2004, 2005; Ziegler and Dèzes 2005).

It is difficult to further constrain the geometry, timing, processes and causes of rifting and of folding, because the present-day structure of the European plate includes interfering signatures of these and older events. The present work is an attempt at resolving this difficulty by separating the respective signatures of each event. This will provide valuable geometrical and chronological constraints, against which models of rifting and of folding may be tested independently.

First, we review the geodynamic history of the NW-Alpine foreland and underline some questions that remain about the rifting and folding events. Second, we review the theoretical geometrical signatures of rifting, of foreland flexural bending, of intraplate buckling and of upwelling asthenospheric thermal anomalies. Then we discuss the present-day crustal geometry of the NW-Alpine foreland on the basis of structure-contour maps compiled for the top of basement and the Moho. From these maps, we identify and remove the rift geometrical signature to produce a structure-contour map for the top of basement as it would be, had rifting not occurred during the Cenozoic. On the basis of this rift-free map, we discuss the geometry and the processes involved in the development of long-wavelength lithospheric folds in the NW-Alpine foreland. Then we place chronological constraints on the rifting and folding events, by analysing the sedimentary and volcanic record of the Upper Rhine Graben. At last, we discuss the development of Cenozoic rifts and lithospheric folds, in relation with the geodynamic history of the western Alpine belt.

Geological setting

Topography

The $1{,}500 \times 1{,}000$ km^2 wide region under study extends from the Armorican Massif (western France) to the Bohemian Massif (Czech Republic) and from the Alpine front to the English Channel and North Sea (Fig. 2). This region includes a number of topographic shields, with elevations commonly higher than +250 m, where pre-Mesozoic basement crops out. These are the Armorican Massif, the Massif Central, the Morvan, the Vosges, the Black Forest, the Rhenish Massif (including the Ardennes, Hunsrück, Taunus, Eifel and Sauerland submassifs) and the Bohemian Massif. Burgundy is a topographic saddle that strikes NE and links the Massif Central to the Vosges; similarly, the Swabian Jura is a subdued topographic ridge that strikes NE from the Black Forest to the Bohemian Massif, and the Vogelsberg–Spessart mountains form a topographic saddle that links the Rhenish and Bohemian Massifs. Early Mesozoic sediments crop out on these three saddles.

The basement shields are separated from each other by wide intracratonic basins with elevations commonly lower than +250 m and where Meso-Cenozoic sediments have been preserved. These are the Flanders, the Netherlands, the North-German Platform, the Paris Basin and the Franconian Basin. A linear subdued trough strikes NE from the Paris Basin to the Franconian Basin, across Lorraine, the northern part of the Upper Rhine Graben and the Jagst Valley.

Southeast of the Burgundy–Swabian Jura topographic ridge, the Molasse Basin is the northern foreland basin of the Alpine mountain belt. The Jura mountains, with elevations of +500 to +1,500 m, are a thin-skinned fold-and-thrust belt that developed during the last 11–3 Ma, at the expense of the outermost part of the Molasse Basin. The ECRIS appears as a system of narrow linear topographic troughs filled with Cenozoic sediments (Eger, Lower Rhine, Upper Rhine, N-Bresse, S-Bresse, Roanne, Limagne, Valence and Lower Rhône Grabens).

Geological history and stratigraphy

The present-day structure of the NW-European plate has resulted from a complex geological history that extends back to Late Paleozoic times. This history includes the growth and decay of the Hercynian mountain belt (Devonian to Permian), the development of a submerged continental platform (Triassic to Middle Jurassic), the opening of the Ligurian Tethys Ocean (Jurassic) and of the North Atlantic Ocean (Early Cretaceous to present), the development of the Alpine mountain belt (Late Cretaceous to

present) and the opening of the ECRIS (Late Eocene to present).

Growth and decay of the Hercynian mountain belt (Devonian to Permian)

The collision of Gondwana with Laurentia led to the development of the Hercynian belt during the Devonian and the Carboniferous. This mountain range extended across the whole area under study, from the Armorican Massif to the Bohemian Massif. Paleozoic rocks that were deformed, metamorphosed and emplaced during this orogeny now crop out on the topographic shields or are covered by Meso-Cenozoic basins.

During the Late Carboniferous and Permian, a widespread system of grabens developed that were filled with continental clastic deposits; important magmatic activity occurred at that time (Ziegler 1990; Ziegler et al. 2004). The grabens have been interpreted as syn- to post-orogenic transtensional gravitational collapse structures (Burg et al. 1994a, b; Ziegler et al. 2004). Some Permian grabens now crop out on the topographic shields, while drilling and geophysical exploration have detected them below Meso-Cenozoic basins (Mégnien 1980; Debrand-Passard 1984; Guillocheau et al. 2000; Ziegler et al. 2004).

We will follow the convention usually adopted in Western Europe by naming "basement" all Paleozoic rocks (either sedimentary, intrusive or extrusive) that were deformed, metamorphosed or emplaced during the Hercynian orogeny, including the Permian grabens and their sedimentary and volcanic infill.

Development of a submerged continental shelf (Early Triassic to Middle Jurassic)

During the Early Triassic, the elevation of the Hercynian belt decreased by a combination of erosional levelling, gravitational collapse and thermal subsidence. Widespread alluvial plains progressively covered the basement with a sequence of continental clastic sediments on average 200 m thick. A 500 m thick sequence including river deposits, alluvial fans, evaporitic facies and littoral to open marine sediments, was deposited during the Middle to Late Triassic. From the Hettangian to the Toarcian, a subsiding mixed carbonate/clastic shelf developed over western Europe and a sequence of marine shales and limestones, on average 500 m in thickness, covered the Triassic deposits (Ziegler 1990; Guillocheau et al. 2000; Ziegler et al. 2004). The development of a sequence of alluvial, coastal and marine carbonate sediments from the Early Triassic to the Middle Jurassic implies that the top of the crust, which had previously been thickened by the Hercynian orogeny, was close to sea-level in most parts of the NW-Alpine foreland at that time.

Tethyan rifting: opening of the Ligurian ocean (Early to Late Jurassic)

During the Early and Middle Jurassic, Africa migrated southeastwards with respect to Europe, in conjunction with the opening of the Central Atlantic Ocean (Dewey et al. 1989; Rosenbaum et al. 2002; Schettino and Scotese 2002). This motion produced oblique continental rifting at the southern border of the European plate. During the Bajocian, oceanic spreading started in the Ligurian Tethys ocean (Schettino and Scotese 2002). The NW-Alpine foreland was then part of a submerged continental shelf open towards this newly forming ocean; a sequence of marine carbonates, on average 1,000 m in thickness, was deposited on the shelf between the Bajocian and the Tithonian, possibly in response to post-rift thermal subsidence (Mégnien 1980; Debrand-Passard 1984; Ziegler 1990; Guillocheau et al. 2000).

North-Atlantic rifting and oceanic spreading (Early Cretaceous to present)

Continental rifting between the American and European plates started in the Early Cretaceous; it was followed, from the Aptian onwards, by oceanic spreading in the North Atlantic (Schettino and Scotese 2002). Rifting and the onset of spreading were contemporaneous with a sharp decrease of the subsidence rate in the Paris Basin (Guillocheau et al. 2000), but southeastern France was still part of a subsiding carbonate shelf open towards the Ligurian Tethys ocean (Debrand-Passard 1984).

Development of the Alpine subduction-collision belt (Late Cretaceous to Present)

During the Aptian, in conjunction with the opening of the South Atlantic Ocean, Africa started to move northeastwards with respect to Eurasia; the Ligurian Tethys ocean started to disappear by subduction (Dewey et al. 1989; Rosenbaum et al. 2002; Schettino and Scotese 2002; Lacombe and Jolivet 2005). Wide parts of the European plate (including the Massif Central, southernmost Lower Rhône Valley, Bresse, Jura, Upper Rhine Graben, Ardennes, Artois, Armorican Massif and Bohemian Massif, Fig. 2) were uplifted at that time; these regions were subjected either to subaerial erosion or to the deposition of thin continental sequences including lacustrine carbonates, fluviatile sediments and alterites (Debrand-Passard 1984; Ziegler 1990; Guillocheau et al. 2000). At the same time, the rate of subsidence increased in the Paris Basin (Guillocheau et al.

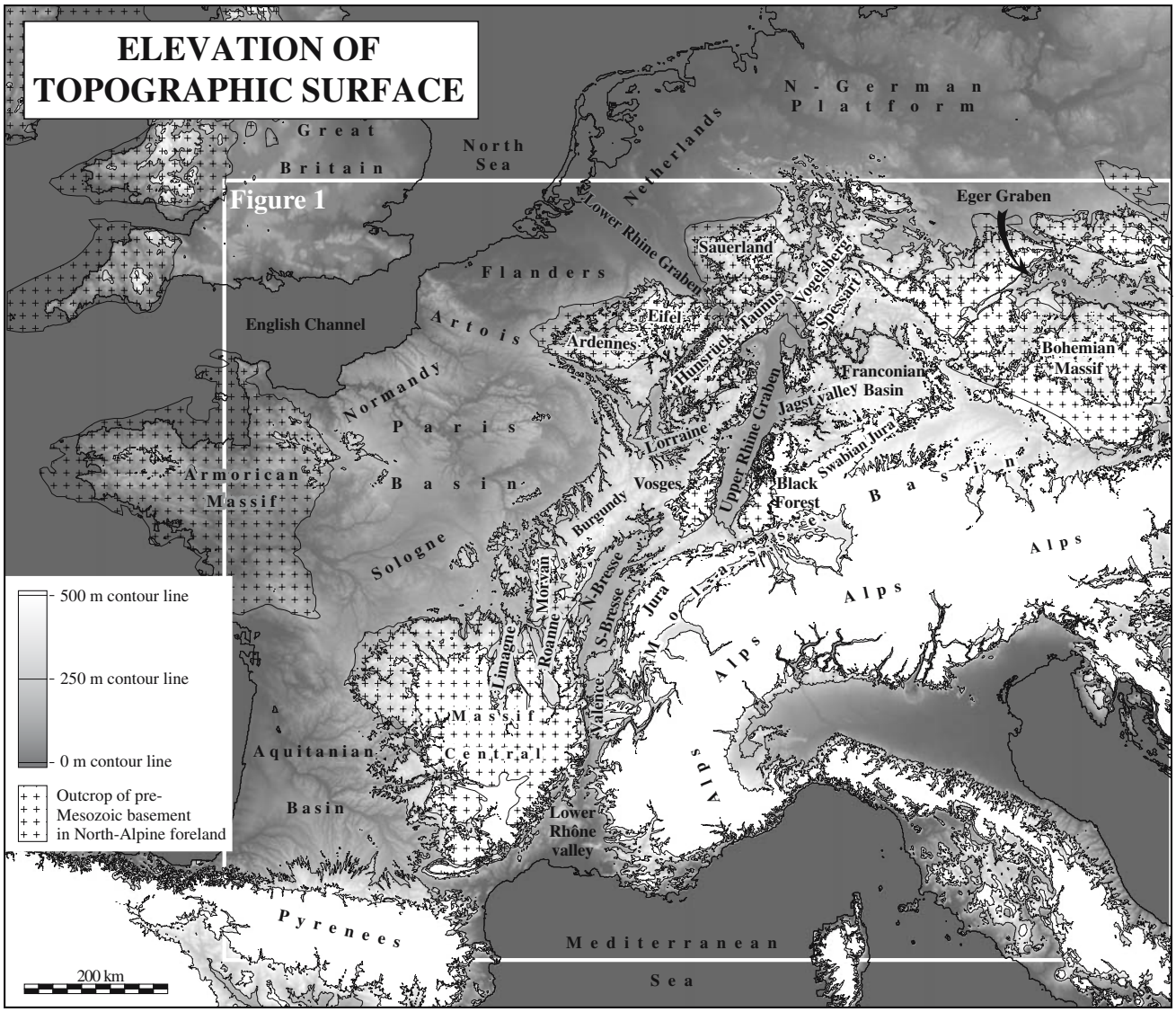

Fig. 2 Topographic map. The NW-Alpine foreland is composed of topographic shields (elevations above +250 m), where the pre-Mesozoic basement crops out, alternating with topographic basins (elevations below +250 m), where Meso-Cenozoic sediments have been preserved. The ECRIS forms a system of linear topographic troughs

2000) and in the central Lower Rhône Valley (Debrand-Passard 1984). Intraplate deformation responsible for these differential vertical motions includes basin inversion, up-thrusting of basement blocks and lithospheric folding (Ziegler 1990; Ziegler et al. 1995; Guillocheau et al. 2000; Dèzes et al. 2004).

In the Paleocene, there were two subduction belts at the southern border of the European plate (Fig. 3a). West of Corsica, the Corsica–Betics–Rif belt was composed of a Tethyan (Ligurian) oceanic domain subducting northwards below thickened Iberian continental crust. This orogenic wedge was associated with a thin-skinned fold-and-thrust belt in its Pyreneean-Provence foreland (Dèzes et al. 2004; Lacombe and Jolivet 2005). Further east, the Alpine belt was composed of a Tethyan (Valaisan) oceanic domain subducting southwards below Adria, a microcontinent initially located between Africa and Europe or linked to Africa. The development of a third subduction belt at the emplacement of the present-day Pyrenees is still debated (Schettino and Scotese 2002; Dèzes et al. 2004; Lacombe and Jolivet 2005).

By Late Eocene, the Valaisan ocean was closed and Adria eventually collided with the European passive margin (Fig. 3c). West of Corsica, the subduction of the Ligurian ocean below Iberia continued (Dèzes et al. 2004; Lacombe and Jolivet 2005).

The Molasse Basin started to develop during the Eocene by flexural bending of the European plate under the weight of the Alpine orogenic wedge (Fig. 3c; Ford et al. 2006). From the Bartonian onwards, the Alpine orogenic wedge and the Molasse Basin progressively migrated towards the

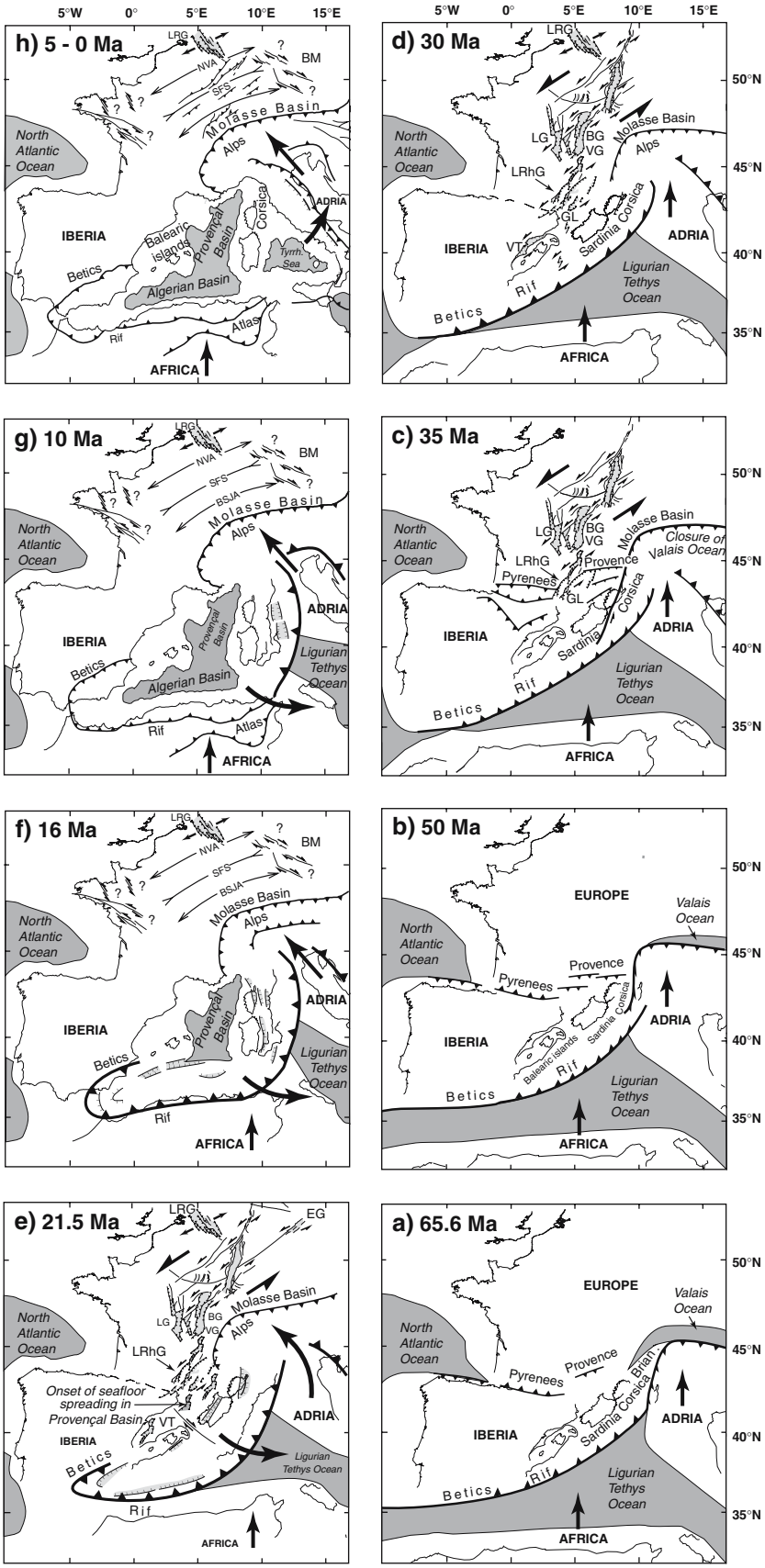

Fig. 3 Structural maps showing the evolution of the Alpine orogen and of its foreland during the Cenozoic. Geodynamic evolution of Mediterranean region after Lacombe and Jolivet (2005); location and geometry of faults in foreland after Dèzes et al. (2004). Development of Jura thin-skinned fold-and-thrust belt (from 11 Ma onwards) not shown for clarity of drawing. *NVA* Normandy–Vogelsberg Anticline, *BSJA* Burgundy–Swabian Jura Anticline, *BG* Bresse Grabens, *BM* Bohemian Massif, *EG* Eger Graben, *GL* Gulf of Lion, *LG* Limagne Graben, *LRG* Lower Rhine Graben, *LRhG* Lower Rhône Grabens, *SFS* Sologne–Franconian Basin Syncline, *VT* Valencia Trough

NW (Fig. 3c–h); the Molasse Basin was filled by a sequence of shallow-marine to continental clastic sediments, up to 5,000 m thick (Burkhard and Sommaruga 1998; Ford and Lickorish 2004; Berger et al. 2005a, b; Ford et al. 2006). The Jura thin-skinned fold-and-thrust belt started to develop 11 Ma ago, at the expense of the outermost part of the Molasse Basin (Laubscher 1986, 1992; Philippe et al. 1996; Becker 2000).

Intraplate deformation of the Alpine foreland (Late Cretaceous to Present)

Not only did the convergence between Africa and Europe produce crustal thickening in mountain belts located at the southern border of the European plate, thin-skinned deformation in their near foreland (Helvetic Subalpine belts, Jura and Provence) and flexural bending of the lithosphere in the Molasse Basin, but it was also responsible for deformation far into the European plate. Jurassic to Early Cretaceous grabens and normal faults were inverted from the Late Cretaceous to the Pleistocene in the Paris Basin, English Channel, southern England, North Sea and northern Germany (Ziegler 1988, 1990; Ziegler et al. 1998; Guillocheau et al. 2000; Dèzes et al. 2004; Ziegler and Dèzes 2005). It has been demonstrated that the Alpine orogeny also entailed long-wavelength intraplate folding of the European lithosphere (Lefort and Agarwal 1996, 2002; Guillocheau et al. 2000; Dèzes et al. 2004). The location, geometry and timing of development of the lithospheric folds are still controversial, however. On the basis of low-pass filtering of gravimetric anomalies, Lefort and Agarwal (1996, 2002) inferred that concentric lithospheric undulations, with a wavelength of 200–300 km and amplitude of 2–4 km, developed around the Alpine front during the Cenozoic. From the stratigraphic record of the Paris Basin, Guillocheau et al. (2000) concluded that NW-striking folds developed during the Early Cretaceous, east-striking folds developed during the Late Cretaceous and NE-striking folds developed during the Late Miocene. Michon and Merle (2001, 2005), Michon et al. (2003) and Bourgeois et al. (2004) attributed part of the uplift of the Rhenish Massif and of the Burgundy–Vosges–Black Forest area to the formation of NE-striking lithospheric anticlines during the Late Cretaceous and Paleocene. In contrast, Dèzes et al. (2004) and Ziegler and Dèzes (2005) propose that uplift started during the Oligocene for the Rhenish Massif and in the Early Miocene (18 Ma) for the Burgundy–Vosges–Black Forest anticline.

Unfortunately, the results of thermochronological studies in the Massif Central, the Vosges, the Black Forest and the Rhenish Massif are unclear. Apatite (U + Th)/He data on samples taken above 500 m in the Vosges and AFT data in the Massif Central are consistent with cooling episodes between the middle Cretaceous and the Paleocene (Barbarand et al. 2001; Bourgeois et al. 2004; Peyaud et al. 2005), whereas AFT and apatite (H + Th)/He data on samples taken at lower elevations in the Vosges and the Black Forest indicate successive cooling episodes in the Late Cretaceous-Paleocene, in the Oligocene and in the Miocene (Link et al. 2003). In the Rhenish Massif, AFT data show a complex pattern of uplift since Late Paleozoic times (Karg et al. 2005), whereas geomorphologic data support 250 m uplift since 0.8 Ma (Garcia-Castellanos et al. 2000; Meyer and Stets 2002; Van Balen et al. 2002).

Opening of the European Cenozoic rift system (Late Eocene to Present)

The ECRIS was activated during the Late Eocene (Fig. 3c). This extensional system extends from the Bohemian Massif to the Mediterranean Sea (Fig. 1). It comprises the Eger, Hesse, Lower Rhine, Upper Rhine, Bresse, Massif Central (Limagne, Roanne, Forez), Valence and Lower Rhône (Alès, Manosque, Camargue) Grabens (Ziegler 1994). Before the opening of the oceanic Provençal Basin of the Mediterranean Sea (21.5 Ma, Dèzes et al. 2004), the ECRIS extended further south, through the Gulf of Lion, along the eastern coast of Spain, and into the Valencia Trough (Fig. 3c–e). The Late Eocene to Pleistocene infill of the grabens comprises continental, lacustrine, fluviatile and shallow marine (brackish and evaporitic) deposits. This sequence reaches a maximal thickness of 3,500 m in the northern part of the Upper Rhine Graben. Moderate volcanic activity occurred in some parts of the ECRIS from the Late Cretaceous to the Pleistocene (Fig. 1; Michon and Merle 2001; Dèzes et al. 2004).

Magnitudes of extensional strain derived from upper crustal faulting amount to about 2–3 km (percentage of crustal extension ρ = 5–10%) across the Limagne Graben, 1–2 km (ρ = 5%) across the Roanne Graben, 2 km (ρ = 10%) across the Bresse Grabens and 7 km (ρ = 25–30%) across the Upper Rhine Graben; upper crustal extension apparently diminishes from 4 to 5 km (ρ = 15%) in the southeastern part of the Lower Rhine Graben to zero in its northwestern part (Dèzes et al. 2004). On the other hand, the amounts of extensional strain computed from the crustal configuration, with the assumption that variations in present-day crustal thicknesses are related to rifting alone, are apparently two to three times greater than the above values (Bergerat et al. 1990; Brun et al. 1992; Geluk et al. 1994; Ziegler 1994; Merle et al. 1998; Dèzes et al. 2004).

The orientation and history of tectonic motions in the ECRIS have generally been inferred from regional paleostress fields computed by statistical analyses of fault-slip data (Bergerat 1987; Merle and Michon 2001; Michon and Merle 2001; Michon et al. 2003; Dèzes et al. 2004, 2005; Michon and Merle 2005; Ziegler and Dèzes 2005). These

various attempts have led to highly diverging interpretations, partly because fault-slip data in the NW-Alpine foreland are poorly constrained in time (Michon and Merle 2005; Dèzes et al. 2005), but also because the orientation of slip on faults reflects the orientation of local relative displacements between tectonic blocks, rather than the orientation of regional stress fields (Gapais et al. 2000).

The timing of rifting has generally been inferred from the preserved sedimentary infill of the grabens (Merle et al. 1998; Merle and Michon 2001; Michon and Merle 2001; Michon et al. 2003; Dèzes et al. 2004; Ziegler and Dèzes 2005). Rifting started in the Late Eocene in the Upper Rhine, Bresse, Massif Central, Valence and Lower Rhône Grabens (Fig. 3c), and propagated northwards (into the Lower Rhine, Hesse and Eger Grabens) and southwards (into the Gulf of Lion and Valencia Grabens) during the Rupelian (Fig. 3d). In the Valencia Trough and in the Gulf of Lion, rifting was followed by the opening of the oceanic Provençal Basin from the Late Aquitanian (21.5 Ma) onwards (Fig. 3e). The southern part of the ECRIS (Valencia Trough, Gulf of Lion, Lower Rhône Valley, Valence Graben) then became inactive; it is not clear whether the northern part of the ECRIS (Bresse, Massif Central, Upper Rhine, Lower Rhine, Hesse and Eger Grabens) became inactive at the same time, or whether these grabens have remained active until the present time. For example, the deposition of up to 400 m of Plio-Pleistocene sediments in the Lower Rhine Graben, in the northern part of the Upper Rhine Graben and in the southeastern part of the Bresse Grabens has been classically interpreted as indicating ongoing rift activity or late tensional reactivation of these grabens (Dèzes et al. 2004; Ziegler and Dèzes 2005). However, other processes, such as northwestward propagation of the Alpine foreland flexural basin (Merle et al. 1998; Michon et al. 2003), or subsidence in lithospheric synclines may account for the deposition of Plio-Pleistocene sediments in some of these grabens. Thus, the sedimentary infill of the grabens probably does not record rifting alone, but also lithospheric folding: rift-related sedimentation may have been reduced on the crests of lithospheric anticlines and enhanced in lithospheric synclines. The signatures of rifting and of folding must be separated before the history of rift development can be addressed.

Geometrical signatures of rifting, foreland flexural bending, intraplate buckling and up-welling asthenospheric thermal anomalies

Rifting

Stretching of the lithosphere leads to lithospheric and crustal thinning (McKenzie 1978). Different modes of thinning are possible, depending on the initial rheological profile of the lithosphere (Buck 1991; Brun 1999; Ziegler and Cloetingh 2004). Stretching of a lithosphere with an initial crustal thickness on the order of 30 km, such as the NW-Alpine lithosphere was before rifting, leads to the formation of narrow rifts. In narrow rifts, the upper part of the crust subsides between normal faults, thus allowing the development of a trough filled by syn-rift sediments; conversely, the base of the crust and the base of the lithosphere rise below the rift axis (Fig. 4a). Heat transfer from the passively uplifting asthenosphere decreases the density of the lithosphere. Thus, the whole lithosphere in and around the rift is bent upwards by regional isostatic uplift (Kooi and Cloetingh 1992; Kusznir and Ziegler 1992). The top of the pre-rift crust rises and can become exposed to erosion on the rift shoulders. The difference in elevation between the rift shoulders and the surrounding regions is accommodated by flexural bending of the lithosphere.

Hence the geometrical signature of a narrow rift generally comprises (1) at the top of the pre-rift crust, a narrow linear trough filled with syn-rift sediments, surrounded by two eroded linear shoulders, the elevation of which decreases asymptotically with increasing distance from the rift axis and (2) at the base of the crust, a linear bulge of rising lithospheric mantle located below the rift axis. The magnitude of uplift of rift shoulders and of the Moho depends on the stretching factor (β) across the graben: under the assumption of a constant extensional strain, narrower grabens are associated with stronger uplifted flanks than wider grabens (Kusznir and Ziegler 1992).

Foreland flexural bending

The development of foreland basins in front of mountain ranges, especially the Alps, has been successfully explained by flexural bending of an elastic lithospheric plate under the weight of an orogenic wedge (e.g. Beaumont 1979; Allen et al. 1986; Allen and Allen 1990; Sinclair et al. 1991; Gutscher 1995; Stewart and Watts 1997; Burkhard and Sommaruga 1998; Watts 2001; Turcotte and Schubert 2002; Leseur et al. 2005). If the lithosphere is assumed to behave elastically, the profile of the flexure corresponds generally to a 3rd order polynomial and includes a 1,000–6,000 m deep foreland basin close to the orogenic front, a 100 to 500 high-forebulge anticline at a distance of 100–300 km from the orogenic front, and a 10–50 m deep backbulge syncline farther in the foreland (Fig. 4b). Parameters controlling the shape of the flexure are (1) the effective elastic thickness of the lithosphere, (2) its elasticity, (3) the magnitude, orientation and location of the forces applied to the lithosphere by the orogenic wedge, (4) the resistance of the asthenosphere.

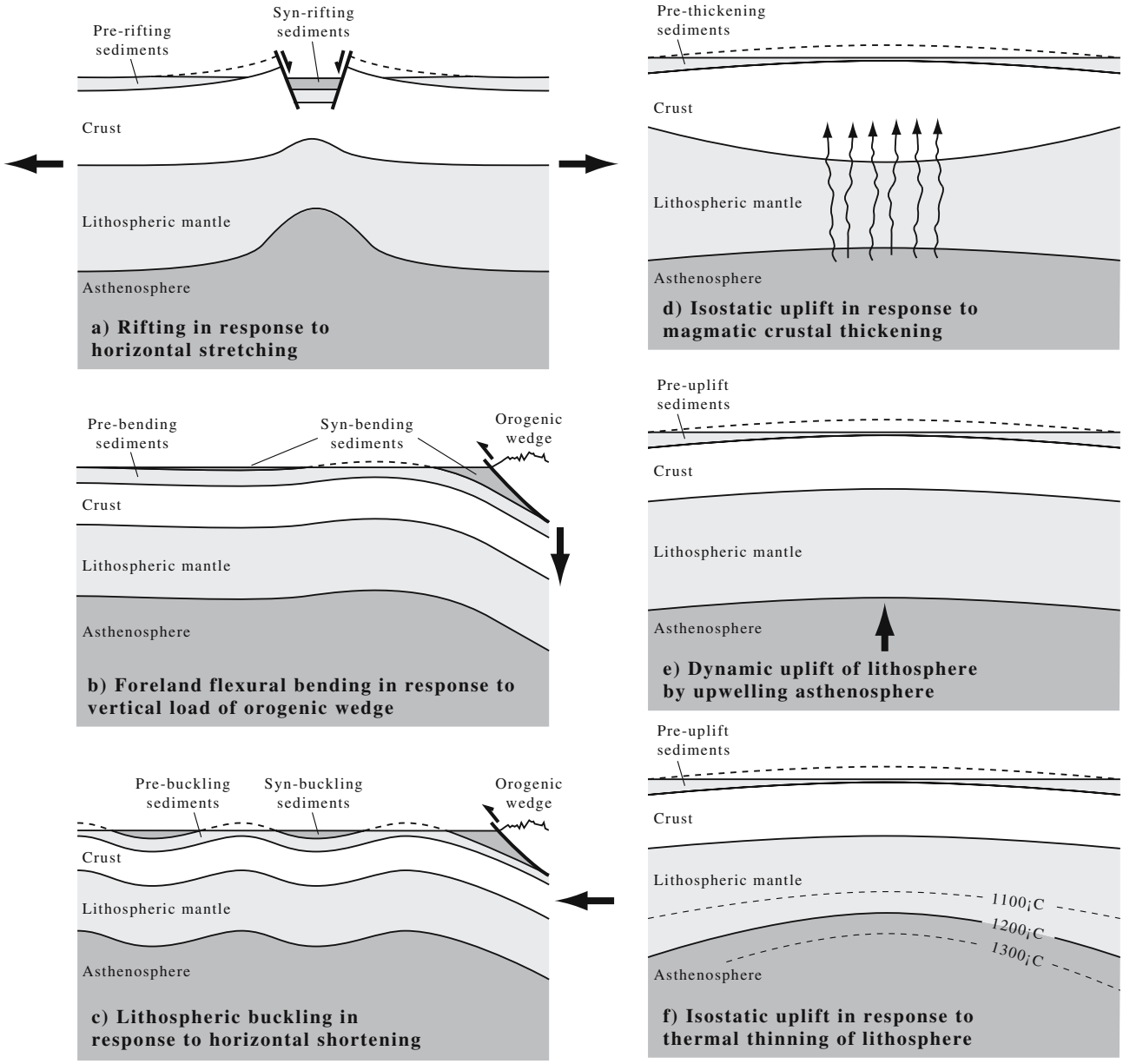

Fig. 4 Sketches (not to scale) of theoretical geometrical signatures of **a** rifting, **b** foreland flexural bending, **c** lithospheric buckling, **d** magmatic crustal thickening, **e** dynamic uplift of lithosphere by upwelling asthenosphere and **f** thermal thinning of lithosphere by asthenospheric thermal anomalies

The upper crustal signature of foreland flexural bending comprises (1) a foreland basin (foredeep) which can be several thousands of metres deep, filled with syn-bending sediments, (2) an arch (forebulge) which can be a few hundreds of metres high, and (3) possibly a shallow basin (backbulge syncline), a few tens of metres deep. The foredeep, the forebulge and the backbulge migrate with time towards the foreland. Syn-bending sediments, if present, are thicker in the backbulge than on the forebulge. Conversely, pre-bending rocks are more deeply eroded on the forebulge than in the backbulge. The base of the crust mimics the foredeep/forebulge/backbulge geometry of the surface.

Intraplate buckling

Some analogue and numerical models suggest that the primary response of the lithosphere to horizontal shortening could be the development of periodic buckle folds (Bull et al. 1992; Martinod and Davy 1992, 1994; Burov et al. 1993; Martinod and Molnar 1995; Ziegler et al. 1995; Gerbault et al. 1999; Cloetingh et al. 1999; Gerbault 2000).

According to these models, lithospheric folds would develop over distances of several thousands of kilometres from plate borders. They could be as much as 3,000 m in amplitude; their wavelength would depend on the rheological profile of the lithosphere, i.e. on the mechanical coupling between the crust and the lithospheric mantle: wavelengths in the order of 200–300 km are generally modelled if the whole lithosphere is involved, whereas wavelengths of 50–100 km are obtained if the crust is fully decoupled from the lithospheric mantle; if the crust is only partially decoupled from the lithospheric mantle, then crustal folds with a wavelength of 50–100 km may possibly be superimposed on lithospheric folds with a wavelength of 200–300 km. Whatever the rheological profile of the lithosphere, buckling of the lithosphere in these models leads to the formation of systems of periodic and parallel synclines and anticlines, which affect both the top and the base of the crust.

Hence the upper crustal signature of intraplate buckle folds is composed of alternating linear troughs and bulges, with amplitudes of several hundreds of metres and wavelengths of 50–300 km (Fig. 4c). Syn-buckling sediments, if present, are thicker in the troughs than on the bulges. Conversely, pre-buckling rocks are more deeply eroded on the bulges than in the troughs. These upper crustal troughs and bulges are spatially coincident with similar periodic troughs and bulges of the Moho.

Actively up-welling asthenospheric thermal anomalies

Actively up-welling asthenospheric thermal anomalies may produce long-wavelength deformation of the lithosphere by three theoretical means. (1) If melting occurs in the asthenosphere, the derived melt may rise upwards and may be added to the crust, thus causing crustal thickening (McKenzie 1984; Cox 1989, 1993). Isostatic equilibrium then requires uplift of the surface of the crust above the thermal anomaly. The geometrical signature of this first process comprises a dome at the surface of the crust, which is spatially coincident with a depression of the Moho (Fig. 4d). The dome and the depression are commonly more or less circular in map view (Cox 1989). (2) The upwelling of anomalously hot asthenosphere may push the lithosphere upwards, thus provoking dynamic uplift and bending of the lithosphere above the anomaly (Lithgow-Bertelloni and Silver 1998; Jones et al. 2002) (Fig. 4e). (3) Thermal erosion of the base of the lithosphere may decrease the average density of the lithosphere, thus generating uplift and bending of the whole lithosphere above the thermal anomaly (Chase et al. 2002). The geometrical signature of the last two processes is a dome both for the top and for the base of the crust (Fig. 4f). The dome is more or less circular in map view.

Present-day crustal geometry in the NW-Alpine foreland

The theoretical geometric signatures of rifting, foreland flexural bending, intraplate buckling and actively up-welling asthenospheric thermal anomalies are different. Thus, analysing the present-day geometry of the base and of the top of the European crust provides constraints on the processes of long-wavelength deformation of the lithosphere in the NW-Alpine foreland. The present-day geometry of these reference levels reflects superimposed deformation possibly produced (1) by the Hercynian orogenic building and collapse, (2) by the Mesozoic rifting and subsequent thermal subsidence, (3) by the Alpine orogeny and (4) by the opening of the ECRIS.

Production of maps

We compiled structure-contour maps for the top-basement and for the Moho, by interpolating digital raster surfaces between control points obtained from several sources (Figs. 5, 6). To draw the top-basement in sedimentary basins, we compiled data from a number of structure-contour maps and seismic profiles available in the literature (Table 1). On topographic shields, where the Meso-Cenozoic cover has not been preserved, we conservatively assumed that the top-basement corresponds to a surface connecting peaks and ridges of the present-day topographic surface. This assumption implies that post-depositional erosion of the Meso-Cenozoic sediments that formerly covered these shields did not cut deep into the basement. The assumption is reasonable because, in cross-section, the surface connecting topographic peaks and ridges on the shields generally prolongs the surface of the basement below the basins (Fig. 7). The interpolation was performed by fitting a surface to the control points, with the tool INTERPOL of the commercial software IDRISI; this tool is commonly used to produce Digital Elevation Models from dense arrays of homogeneously distributed control points.

The Moho map (Fig. 5) is based mainly on the map compiled by Dèzes et al. (2004), with additions and modifications where finer data were available (Table 1). The interpolation was performed by fitting a Triangular Irregular Network to the control points, with the tools TIN and TINSURF of the commercial software IDRISI; these tools are commonly used to produce Digital Elevation Models in regions where control points are sparse or distributed irregularly.

From the spatial distribution of control points, we estimate that the horizontal precision of the compiled maps is better than 1 km for the basement and better than 10 km for the Moho. From the differences observed in the elevations given by different sources for the same control

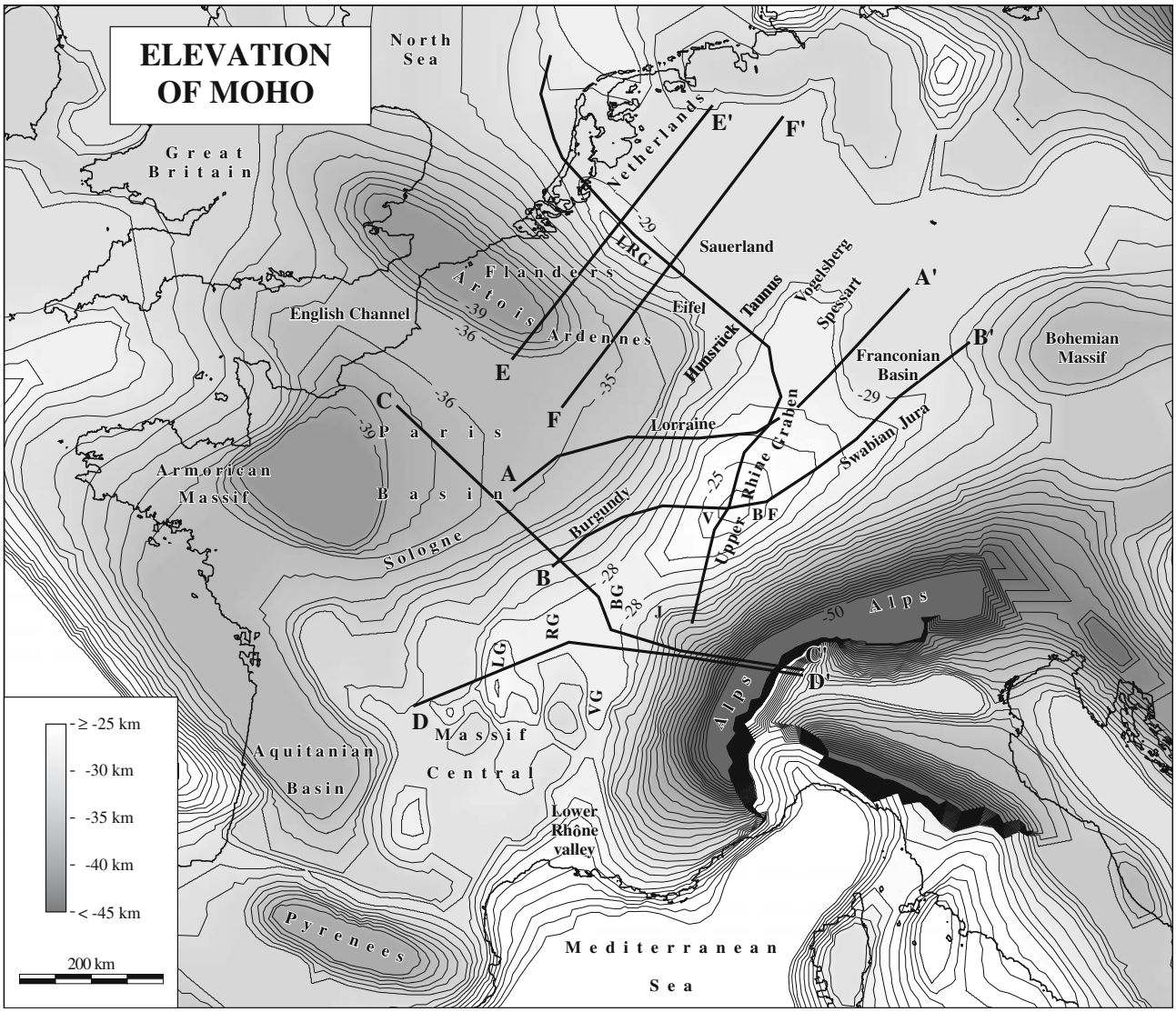

Fig. 5 Contoured elevation map of the Moho in the NW-Alpine foreland (adapted from Dèzes et al. 2004). *Thick black lines*: location of cross-sections (Figs. 7, 8, 13). *BF* Black Forest, *BG* Bresse Grabens, *J* Jura fold-and-thrust belt, *LG* Limagne Graben, *LRG* Lower Rhine Graben, *RG* Roanne Graben, *V* Vosges, *VG* Valence Graben

point, we estimate that the vertical precision is on the order of 100 m for the basement and 1 km for the Moho.

Preliminary qualitative interpretation of maps

Rifts

In the Lower Rhine, Upper Rhine, Bresse, Massif Central and Lower Rhône Grabens, the top-basement defines narrow linear troughs, bordered by linear shoulders, the elevation of which decreases with increasing distance to the rift axis (Fig. 6). The troughs are filled with Cenozoic sediments, whereas the Mesozoic cover has been partly or totally eroded on the shoulders. The troughs are spatially coincident with bumps of the Moho (Fig. 5). Linear troughs on the top-basement, correlated with bumps of the Moho, indicate crustal thinning related to stretching of the lithosphere (Fig. 4a). Thus, these structures are the crustal signature of rifting.

Lithospheric folds

From the Massif Central to the Bohemian Massif, across Burgundy, the Vosges, the Black Forest and the Swabian Jura, the basement defines a ridge that strikes NE and that rises up to more than 0 m (Fig. 6). This ridge is spatially coincident with a linear bulge where the Moho rises up to more than –28 km (Fig. 5).

Below the Rhenish Massif and the Vogelsberg–Spessart mountains, the top-basement defines a NE-striking ridge,

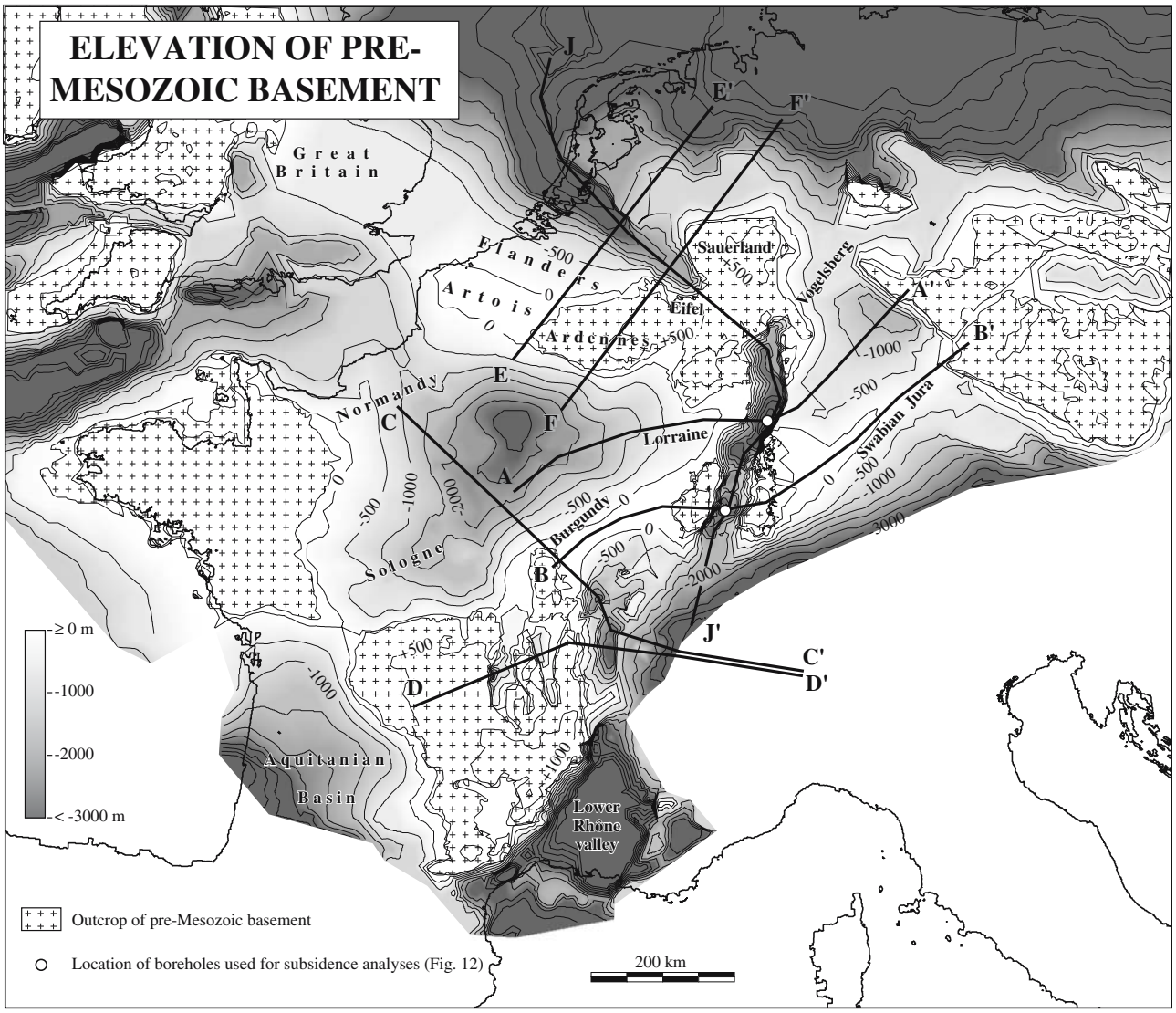

Fig. 6 Contoured elevation map of the top of the pre-Mesozoic basement in the NW-Alpine foreland (for construction see text). *Thick black lines*: location of cross-sections (Figs. 7, 8, 13). Open circles: location of boreholes used for subsidence analyses (Fig. 12)

the elevation of which decreases northeastwards from +500 m on the Rhenish Massif to –1,000 m below the Vogelsberg–Spessart mountains. This ridge coincides spatially with a NE-striking ridge of the Moho, the elevation of which decreases from –28 km on the Rhenish Massif to –30 km below the Vogelsberg–Spessart mountains.

The elevation of the basement is –3,000 m in the deepest part of the Paris Basin and –1,500 m in the deepest part of the Franconian Basins (Fig. 6). A linear trough striking NE, where top-basement elevation remains below 0 m, joins these basins across the northern part of the Upper Rhine Graben. This linear trough is parallel to the Burgundy–Swabian Jura and Rhenish Massif–Vogelsberg ridges.

Southeast of the Burgundy–Swabian Jura ridge, below the Molasse Basin, the top-basement and the Moho deepen down to –4,000 m and to less than –50 km, respectively. North of the Rhenish Massif–Vogelsberg ridge, below the N-German platform and the Netherlands, the top-basement and the Moho drop down to –5,000 m and –31 km, respectively.

In conclusion, two top-basement ridges striking NE, that are spatially coincident with two Moho ridges (Burgundy–Swabian Jura and Rhenish Massif–Vogelsberg) alternate with three top-basement depressions that are spatially coincident with Moho depressions (Molasse Basin, Paris Basin–Franconian Basin, N-German Platform–Netherlands). The Meso-Cenozoic cover has been deeply eroded along the ridges, whereas it has been partly or totally preserved in the intervening troughs. This pattern indicates neither crustal thinning (Fig. 4a) nor crustal thickening (Fig. 4d), but lithospheric folding (Figs. 4b, c, e, f).

Table 1 Sources of data used for compilation of maps of top of basement and Moho (Figs. 4, 5)

Location	Basement	Moho
Paris Basin	Chantraine et al. (1996), Mégnien (1980)	Dèzes et al. (2004)
SE-France	Chantraine et al. (1996), Debrand-Passard (1984)	Dèzes et al. (2004)
Massif Central and Bresse Grabens	Chantraine et al. (1996), Bergerat et al. (1990), Michon (2000)	Bergerat et al. (1990), Zeyen et al. (1997), Dèzes et al. (2004)
Upper Rhine Graben	Munck and Sauer (1979), Ziegler (1990)	Brun et al. (1992), Prodehl et al. (1992), Rousset et al. (1993), Dèzes et al. (2004)
Jura mountains and western Molasse Basin	Burkhard and Sommaruga (1998), Sommaruga (1999)	Burkhard and Sommaruga (1998), Dèzes et al. (2004)
Lower Rhine Graben, English Channel, North Sea, Northern Germany, Franconian Basin, Swabian Jura, eastern Molasse Basin, Alps, Italy, Mediterranean Sea	Ziegler (1990)	Dèzes et al. (2004)

Thickened crust

Below the Ardennes, the Artois and SE-England, the basement defines a WNW-striking bulge, known as the London–Brabant ridge (Fig. 6). Below this ridge, the Moho drops down to –40 km (Figs. 5, 7c), which indicates crustal thickening. The lack of Meso-Cenozoic volcanism indicates that this ridge is not related to post-Permian magmatic crustal thickening (Fig. 4d), but most probably to incomplete re-equilibration of crustal thickness after the Hercynian orogeny. This interpretation is consistent with the pinch-out of Triassic, Jurassic and Cretaceous sediments along the borders of the Ardennes and the Artois, which suggests that this NW-striking ridge remained emerged during the Mesozoic (Ziegler 1990).

Quantitative separation of rifting and lithospheric-folding signatures

Qualitative interpretation of Moho and top-basement geometries suggests that the present-day crustal configuration of the NW-Alpine foreland records interfering signatures of rifting, lithospheric folding and crustal thickening. We now separate quantitatively these signatures. First we identify the rift geometrical signature on the map of the basement, then we remove it; in doing so, we extract the signatures of folding and crustal thickening by producing a rift-free structure-contour map for top-basement as it would be, had rifting not occurred during the Cenozoic.

Determination of rift signature

Upper Rhine Graben

Two crustal sections across the Upper Rhine Graben are displayed in Fig. 7. These sections were drawn along curved lines striking NE (Figs. 5, 6), so as to avoid disturbances caused by the NE-striking lithospheric folds identified on top-basement.

On the southern section (B-B′) that follows the crest of a lithospheric anticline, the top-basement is at an elevation of 0 m in Burgundy and in the Swabian Jura, i.e. in the regions not affected by rifting; the basement rises up to +1,500 m in the Vosges and Black Forest, i.e. on the graben shoulders; it drops down to –3,000 m in the graben. In the northern section (A-A′), that follows the hinge line of a lithospheric syncline, the graben, its shoulders and the regions not affected by rifting all together are 1,500 m lower than in the southern section (B-B′). However, the overall cross-sectional shape of the graben is the same in both sections: the first order cross-sectional signature of the Upper Rhine Graben comprises a 3,000 m deep trough, bordered by symmetrical shoulders, the elevation of which decreases from 1,500 m near the graben to 0 m at a distance of 300 km (Fig. 7, A-A′ and B-B′, Fig. 8, F-F′). The ratio between the amount of shoulder uplift and the amount of graben floor subsidence is 1/2. The ratio between shoulder height and shoulder width is 1/200. The observed uplift of the Moho below the rift is 7,000 m. All these vertical displacements are equal in the northern and southern parts of the Upper Rhine Graben.

In a full (symmetrical) graben, the percentage of crustal extension ρ is given by:

$$\rho = (h_0 - h_1)/h_0, \quad (1)$$

where h_0 and h_1 are the initial and final crustal thicknesses, respectively. The percentage of crustal extension ρ computed from cross-sections A-A′ and B-B′ (Fig. 7) with Eq. (1) is 30% for the Upper Rhine Graben, which is consistent with the value derived from upper crustal faulting by earlier authors (Dèzes et al. 2004).

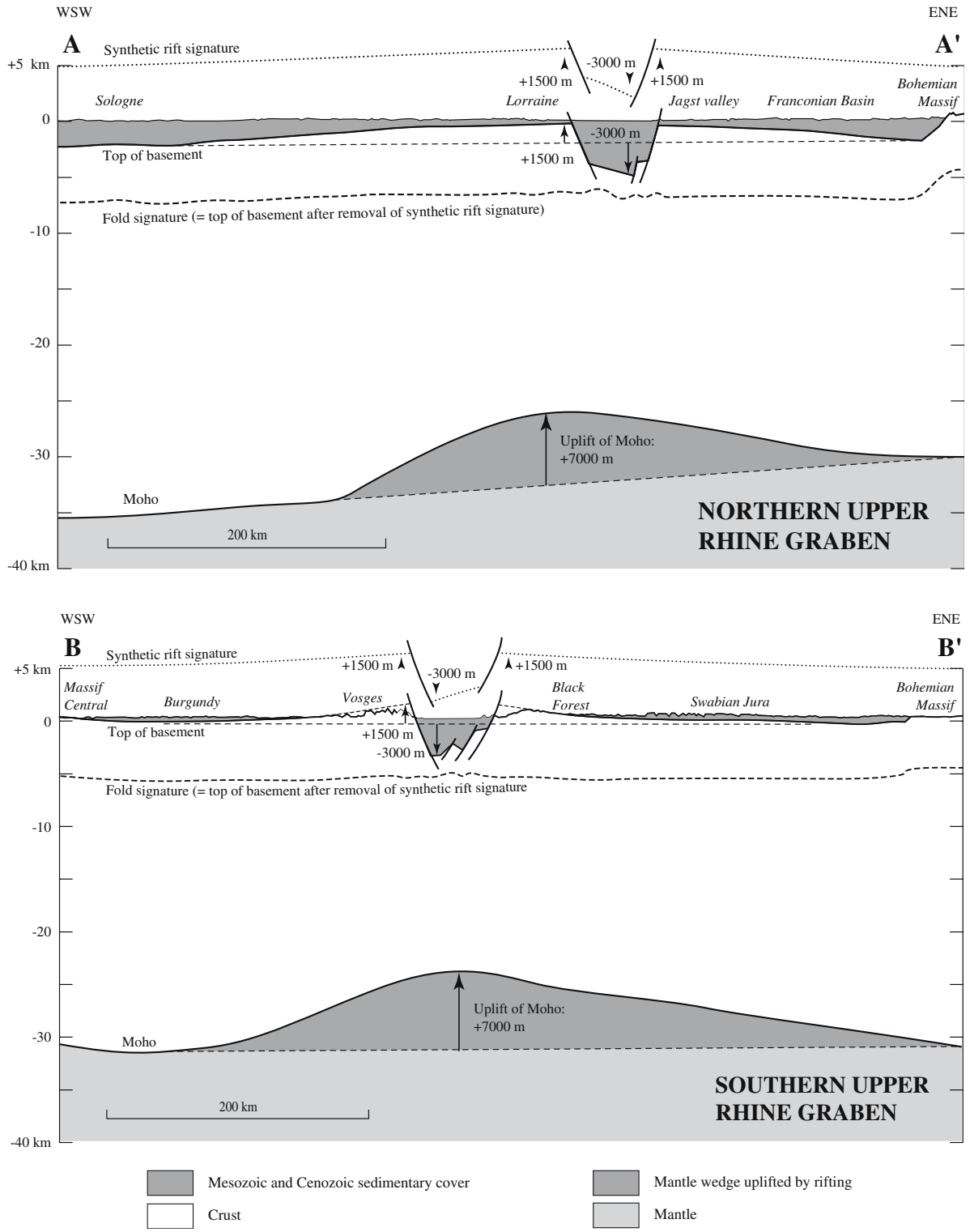

Fig. 7 Crustal sections showing the topographic surface, the Meso-Cenozoic sedimentary cover (*grey shading*), the top-basement and the Moho across the northern (A-A′) and southern (B-B′) Upper Rhine Graben, the Bresse (C-C′) and Massif Central (D-D′) Grabens and the western (E-E′) and eastern (F-F′) Lower Rhine Graben (locations on Figs. 5, 6). *Dotted line* above each section is synthetic rift signature inferred from the actual section; *bold stippled line* is fold signature, i.e. geometry of basement after synthetic rift signature has been subtracted from actual geometry of basement top. For clarity, the synthetic rift signatures and computed fold signatures have been translated vertically by +5 km and –5 km, respectively

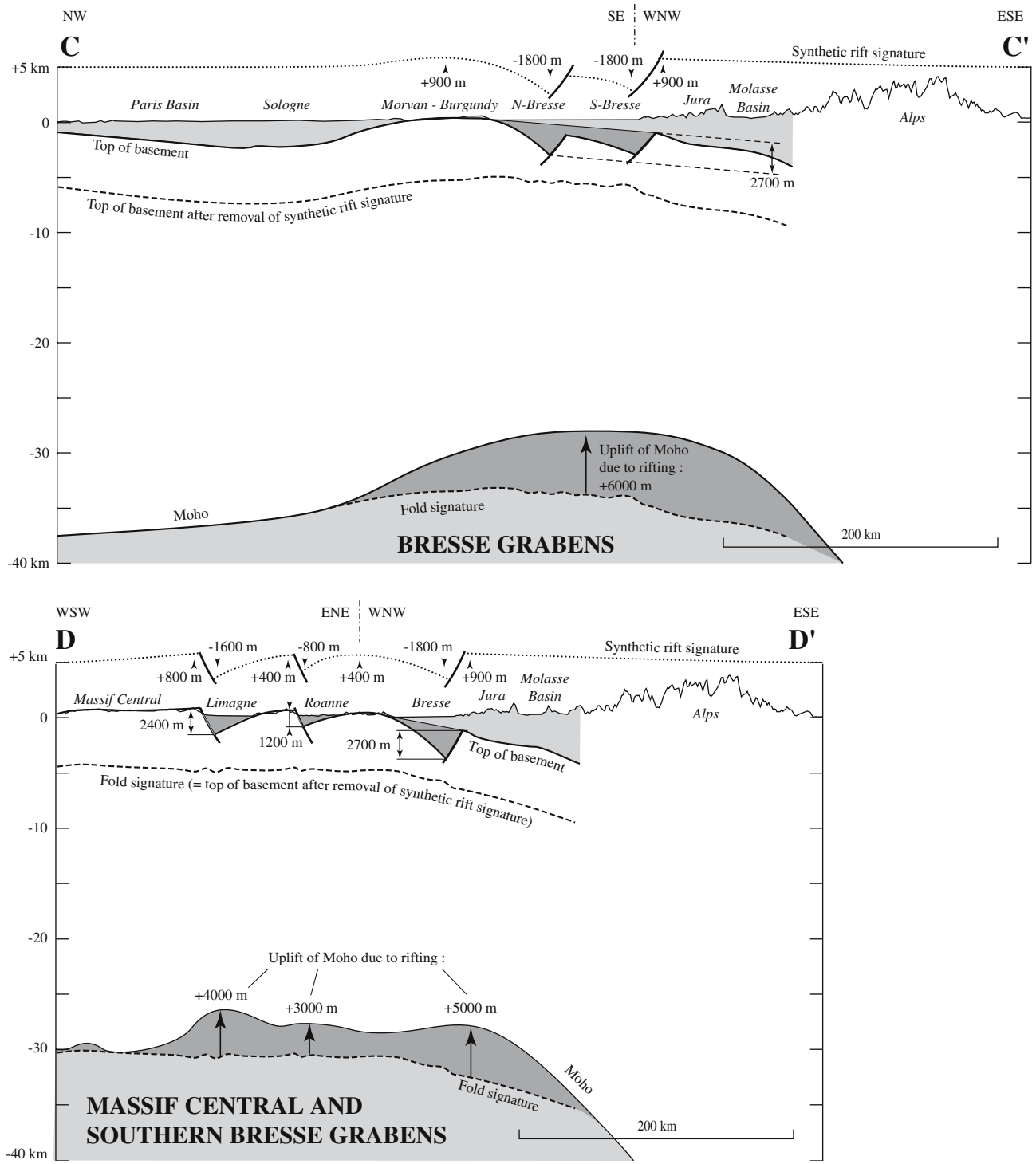

Fig. 7 continued

Bresse and Massif Central Grabens

The Bresse Grabens are east-dipping half-grabens, while the Roanne and Limagne Grabens are west-dipping half-grabens (Fig. 7, C-C′ and D-D′). Vertical offsets of top-basement between graben floors and shoulders are 2,700 m for the Bresse Grabens, 1,200 m for the Roanne Graben and 2,400 m for the Limagne Graben. If ratios between floor subsidence, shoulder uplift and shoulder width are assumed to be the same for these grabens as for the Upper Rhine Graben, the rift signature of the Bresse Grabens comprises two 1,800 m deep trough, bordered by 900 m

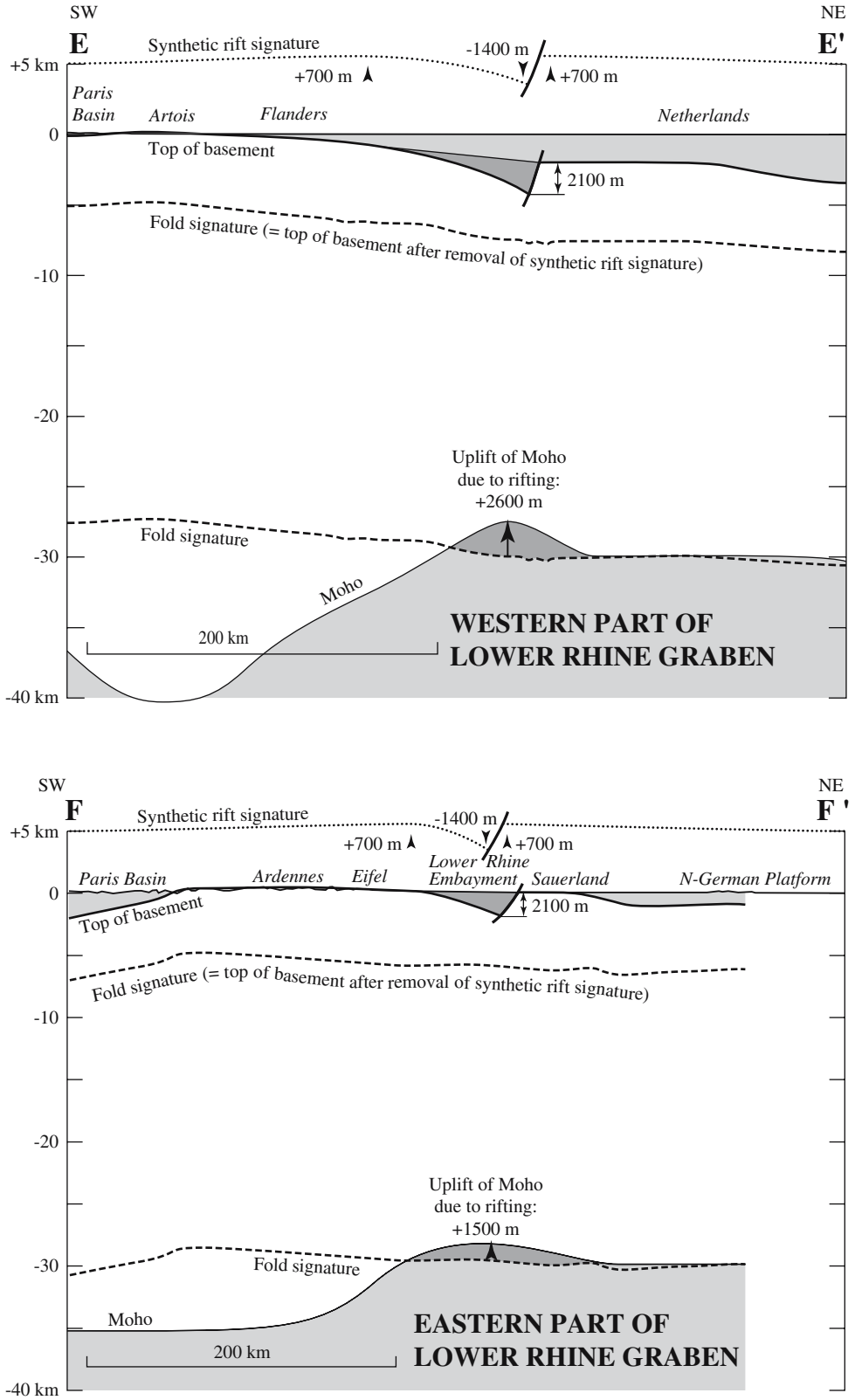

Fig. 7 continued

high shoulders. The Roanne Graben is a 800 m deep trough bordered by 400 m high shoulders and the Limagne Graben is a 1,600 m deep trough bordered by 800 m high shoulders. The Moho was uplifted by 6,000 m below the Bresse Grabens, by 3,000 m below the Roanne Graben and by 4,000 m below the Limagne Graben.

In a half-graben, the cross-sectional surface area of the sedimentary basin and of the uplifted mantle wedge are half the cross-sectional surface area they would have in a full (symmetrical) graben with equivalent amounts of top-basement offset and of Moho uplift. Hence the percentage of crustal extension ρ in half-grabens is given by:

$$\rho = (h_0 - h_1)/(2h_0), \quad (2)$$

where h_0 and h_1 are the initial and final crustal thicknesses in the graben, respectively. The percentage of crustal extension ρ computed from cross-sections C-C′ and D-D′ (Fig. 7) with Eq. (2) are 10, 5 and 10–15% for the Limagne, Roanne and Bresse Grabens, respectively. These values are consistent with those derived from upper crustal faulting by earlier authors (Dèzes et al. 2004).

Lower rhine graben

The Lower Rhine Graben is a northeast-dipping half-graben; rifting entailed 2,100 m of offset between the graben floor and its shoulders (Fig. 7, E-E′ and F-F′). The uplift of the Moho is 1,500–2,600 m. If ratios between floor subsidence, shoulder uplift and shoulder width are assumed to be the same for this graben as for the Upper Rhine Graben, the rift signature of the Lower Rhine Graben comprises a 1,400 m deep trough bordered by 700 m high shoulders. The corresponding percentage of crustal extension ρ, computed from cross-sections E-E′ and F-F′ (Fig. 7) with Eq. (2) is on the order of 10%, which is consistent with the value derived by earlier authors from upper crustal faulting (Dèzes et al. 2004).

Synthetic 3D model of rift signature

From the individual cross-sectional signatures of the grabens, we produced a synthetic 3D geometrical model for the top-basement signature of the central part of the ECRIS. To constrain the model, we projected the individual cross-sectional signatures of the grabens (Fig. 8, cross-sections C-C′, D-D′, E-E′) along the strike of their border faults. Local adjustments of the depth of graben floors were made to take into account their fine-scale structure, which includes second-order horsts, grabens and tilted blocks. For example, the depocentre was placed along the western border fault in the southern part of the Upper Rhine Graben, whereas it was placed along the eastern border fault in its northern part (Brun et al. 1992). We interpolated a digital raster surface between all the grabens and thus we obtained a synthetic structure-contour map for the 3D geometrical signature of the ECRIS on top-basement (Fig. 8). On this map, the shoulders of the grabens form an overall bulge, 400–600 km wide, around the ECRIS.

Subtraction of rift signature

By subtracting the elevation of each pixel in the synthetic model of rift signature (Fig. 8) from the elevation of the same pixel in the actual map of the basement (Fig. 6), we produced an elevation map for the top-basement, as it would be now, had rifting not occurred during the Cenozoic (Fig. 9). On this map, graben troughs and shoulders have been levelled; this demonstrates that the amounts of graben subsidence and shoulder uplift introduced in the 3D model of rift signature are consistent with each other. Small-size bumps and depressions remain in some grabens, particularly in the Lower Rhine Graben. These are related to fine-scale structures that were inaccurately defined or poorly located in the synthetic model of rift signature. These bumps and depressions are sufficiently small in amplitude and wavelength, however, that they do not mask long wavelength and large amplitude deformation of the basement.

Signature of lithospheric folding

Description of folds

Four structures indicative of lithospheric folding appear on the map of the rift-free basement (Figs. 9, 10). These structures are parallel to the Alpine front. (1) The Molasse Basin is a monocline that dips southeast below the Alpine front. The basement is at –4,500 m depth in the deepest part of the basin. (2) An anticline strikes NE from Burgundy to the Swabian Jura, across the Vosges and the Black Forest. The basement is at –500 to 0 m depth along the hinge line of this anticline. (3) A syncline strikes NE from the Paris Basin to the Franconian Basin. The basement is at –1,500 to –3,000 m depth along the hinge line of this syncline. (4) An anticline strikes NE from the Ardennes to the Vogelsberg. The basement is at 0 to –500 m depth along the hinge line of this anticline.

The cross-sectional structure of the folds in the region of the Upper Rhine Graben, a region much affected by rifting, is similar to their cross-sectional structure in the eastern part of the Franconian Basin, a region not much affected by rifting: the folds are 270 km in wavelength and 1,500 m in amplitude in both areas (Fig. 10, cross-sections G-G′ and H-H′). This similarity indicates that the folds are approximately cylindrical. Cross-section C-C′ (Fig. 10) shows how

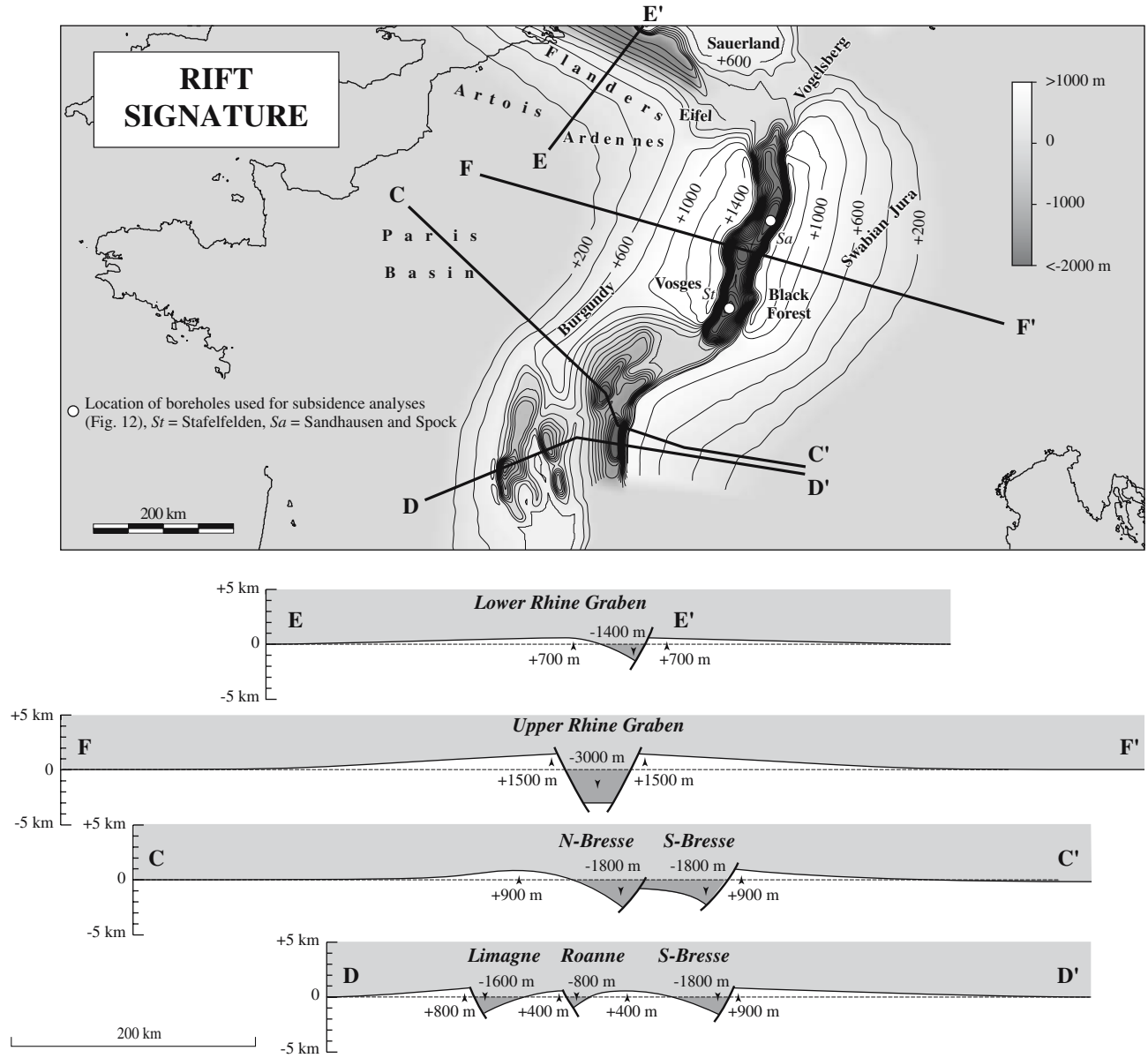

Fig. 8 Map and cross-sections of rift signature on top-basement in the NW-Alpine foreland. Contours indicate amounts of vertical motions of the basement caused by rifting. Positive values indicate uplift (graben shoulders) and negative values indicate subsidence (graben floors). The map was obtained by projecting the cross-sectional signature of each graben (Fig. 7) along strike and by interpolating a raster surface between the grabens. *Open circles*: location of boreholes used for subsidence analyses (Fig. 12)

these cylindrical folds, when prolonged (with same wavelength and amplitude) further west into France, provide an explanation for (1) the Cenozoic uplift of Burgundy and Morvan, (2) the syn- to post-Burdigalian development of a NE-trending synform in the southeastern part of the Paris Basin (Sologne–Pays d'Othe–Lorraine) and (3) the coeval uplift of the northwestern part of the Paris Basin (Champagne–Picardie–Normandie) (Guillocheau et al. 2000).

In the Paris Basin, the cross-sectional geometry of the top-basement (after removal of the rift signature) differs, however, from the fold signature determined further east (Fig. 10, cross-section C-C′). This suggests that the Paris Basin did not only develop by lithospheric folding parallel to the Alpine front. Additional processes are required to explain greater subsidence in the Paris Basin than in the Franconian Basin. This is consistent with the existence of Triassic and Jurassic depocentres extending from the centre of the Paris Basin to Lorraine (Fig. 9; Ziegler 1990; Guillocheau et al. 2000). Previous studies also indicate that the Paris Basin developed by a mixture of stretching and thermal subsidence during the Triassic and the Jurassic, and subsequently by several events of lithospheric folding

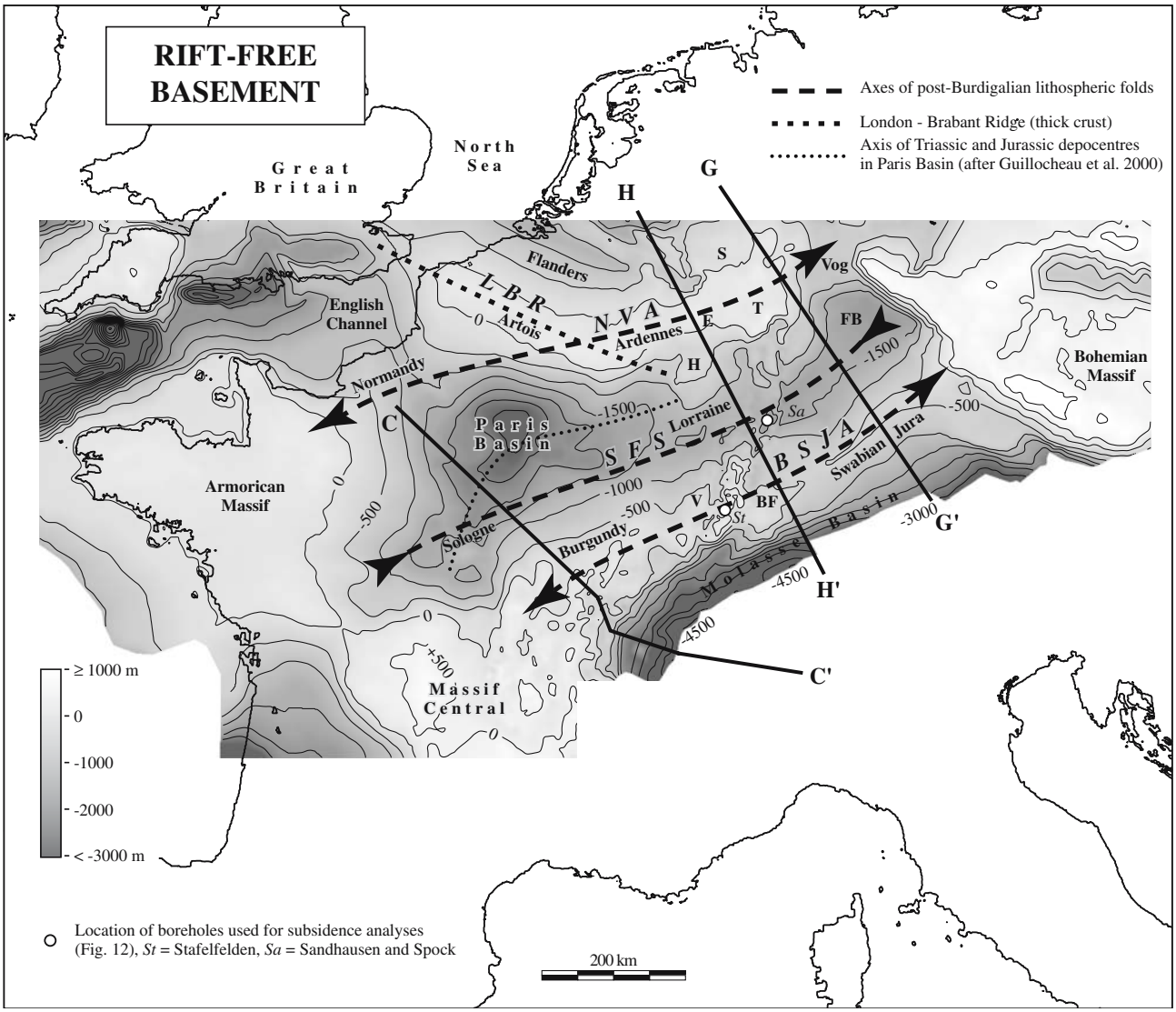

Fig. 9 Map of elevation of basement in the NW-Alpine foreland, with rift signature removed. The map was computed by subtracting the map of rift signature (Fig. 8) from the map of actual elevation of the basement (Fig. 6). *Thick black lines*: location of cross-sections (Fig. 10). *Open circles*: location of boreholes used for subsidence analyses (Fig. 12). *BSJA* Burgundy–Swabian Jura Anticline, *LBR* London–Brabant Ridge (thick crust), *NVA* Normandy–Vogelsberg Anticline, *SFS* Sologne–Franconian Basin Syncline, *BF* Black Forest, *E* Eifel, *FB* Franconian Basin, *H* Hunsrück, *S* Sauerland, *T* Taunus, *V* Vosges, *Vog* Vogelsberg

from the Early Cretaceous to the present-day (Guillocheau et al. 2000; Ziegler et al. 2004).

In conclusion, structures indicative of lithospheric folding on the map of rift-free basement are (1) the Burgundy–Swabian Jura Anticline, (2) the Sologne–Franconian Basin Syncline and (3) the Normandy–Vogelsberg Anticline. A ridge striking WNW remains between the Ardennes and the Artois after removal of the rift signature (Fig. 9). The strong depression of the Moho in this region (Figs. 5, 7c) indicates that this top-basement ridge is not related to lithospheric folding, but to incomplete re-equilibration of crustal thickness after the Hercynian orogeny, as discussed earlier.

Folding process

The parallelism between the observed lithospheric folds and the Alpine front suggests that the folds developed in response to the convergence between Adria and Europe. The cross-sectional shape of the folds is inconsistent with that of folds produced by elastic bending of the lithosphere under the weight of the Alps (Fig. 11). On the other hand, the observed folds are consistent with the results of analogue and numerical models, where horizontal shortening of the lithosphere produces periodic buckle folds (Martinod and Davy 1992, 1994; Martinod and Molnar 1995; Gerbault et al. 1999; Cloetingh et al. 1999; Gerbault 2000).

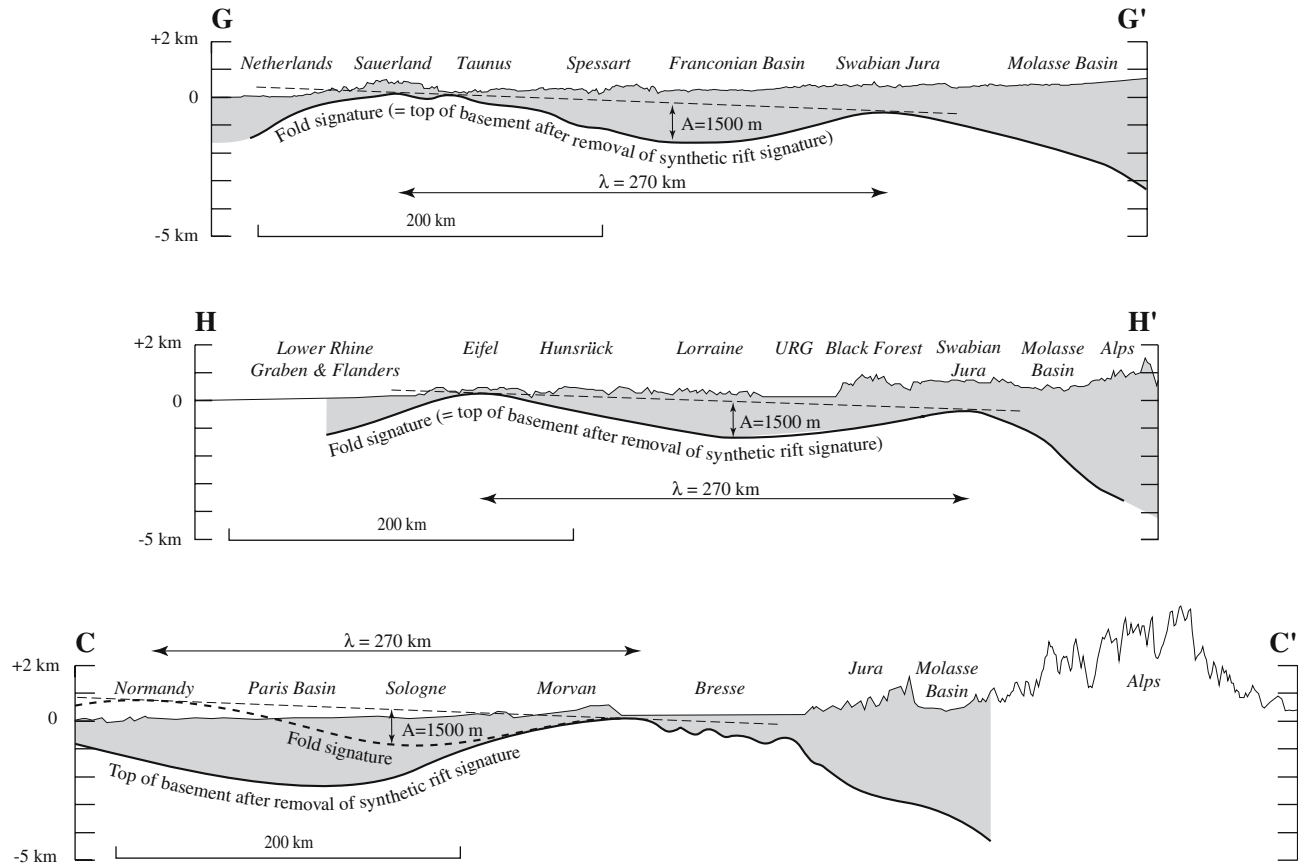

Fig. 10 Cross-sections of top-basement in the NW-Alpine foreland, with rift signature removed (locations on Fig. 9). *Thin line*: actual topographic surface. *Bold line*: elevation of top-basement as it would be, had rifting not occurred. Fold signatures are similar (wavelength = 270 km and amplitude = 1,500 m) in the Franconian Basin (cross-section G-G′) and in the Upper Rhine Graben area (cross-section H-H′). In the Paris Basin, development of folds with assumed same wavelength and amplitude (*bold stippled line* in cross-section C-C′), implies subsidence of Sologne and uplift of Normandy; additional subsidence processes are required to explain the geometry of the basement in the Paris Basin

Wavelengths on the order of 270 km and amplitudes on the order of 1,500 m are obtained in models of buckling, when the crust is not decoupled from the mantle. Hence the observed folds are consistent in azimuth, wavelength and amplitude, with buckle folds produced by horizontal shortening of the whole lithosphere, in response to the NW-directed convergence between Adria and Europe.

The basement deepens sharply from the hinge line of the Burgundy–Swabian Jura Anticline towards the Molasse Basin (Fig. 10). This profile is inconsistent with lithospheric buckling (Fig. 11). On the other hand, models of flexural bending of the lithosphere under the weight of orogenic wedges account for the geometry of this monocline (Fig. 11; Sinclair et al. 1991; Gutscher 1995; Stewart and Watts 1997; Burkhard and Sommaruga 1998; Leseur et al. 2005). According to these models of foreland flexural bending, the development of a foredeep in the Molasse Basin was accompanied by the development of a *ca.* 200 m high forebulge at the emplacement of the Burgundy–Swabian Jura Anticline (Fig. 11). Thus, a small part of the uplift of the Burgundy–Swabian Jura Anticline can be attributed to foreland flexural bending prior to buckling.

Interference patterns

Vosges–Black Forest Massif

In the Vosges–Black Forest Massif, the topographic surface and the top-basement form an approximately circular dome, which is split apart by the URG (Figs. 2, 6). The Moho also forms an approximately circular bump below this region (Fig. 5). After removal of rift signature however, the circular dome disappears from the map of top-basement, leaving the NE-striking Burgundy–Swabian Jura Anticline (Fig. 9). Thus, in accordance with Dèzes et al. (2004), we conclude that the crustal dome below the Vosges–Black Forest area is due to interference between a linear lithospheric anticline striking NE and a linear graben striking NNE.

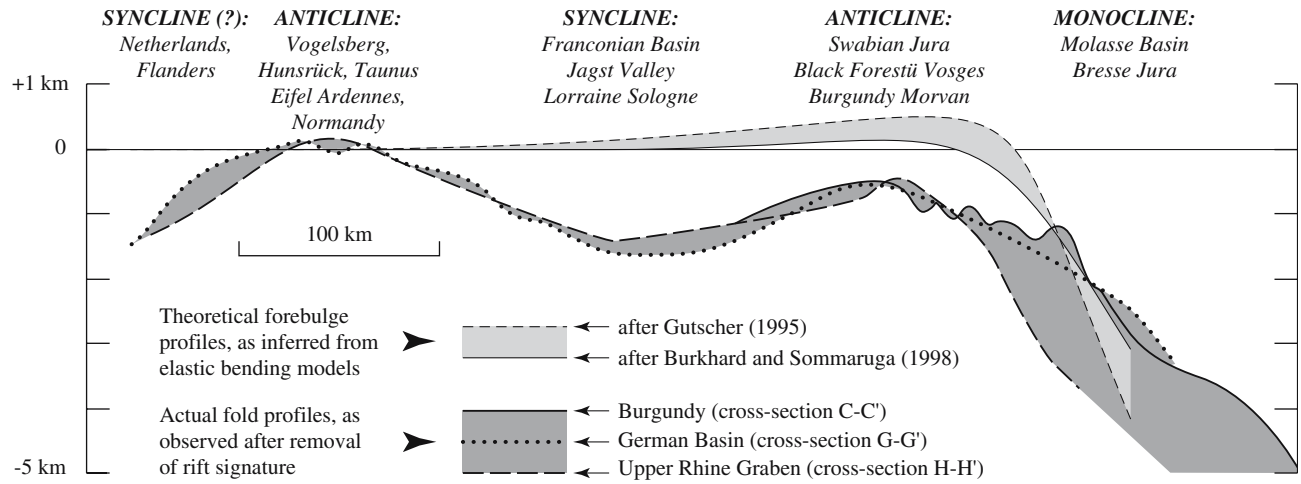

Fig. 11 Profiles of folds observed in the NW-Alpine foreland (Fig. 10) compared with theoretical profiles of folds produced by foreland flexural bending (Gutscher 1995; Burkhard and Sommaruga 1998). The geometry of the Molasse Basin monocline is consistent with foreland flexural bending under the weight of the Alpine orogenic wedge. On the other hand, the geometry of folds observed between the Burgundy–Swabian Jura Anticline and the Normandy–Vogelsberg Anticline is consistent with buckle folds produced by horizontal shortening of the European lithosphere

Rhenish Massif

In the Rhenish Massif, the topographic surface and the top-basement form an approximately circular dome (which is split apart by the URG and LRG), with a linear appendix extending westwards into the region of thickened crust below the Ardennes and Artois (Figs. 2, 6). Below the Rhenish Massif itself (Eifel, Sauerland, Hunsrück, Taunus and Vogelsberg), the Moho rises above –30 km (Fig. 5). High elevations of the topographic surface, top-basement and Moho in the Rhenish Massif have classically been interpreted as evidence for thermal thinning or for dynamic uplift of the lithosphere by asthenospheric thermal anomalies (Fig. 2e, f; Garcia-Castellanos et al. 2000; Dèzes et al. 2004). This interpretation is apparently supported by the occurrence in this region of (1) Cenozoic volcanic activity, (2) thin lithosphere and (3) a seismic velocity anomaly in the asthenosphere (Babushka and Plomerova 1992; Ritter et al. 2001; Keyser et al. 2002).

However, after removal of the rift signature from the map of top-basement, the circular dome is strongly attenuated, leaving mostly the NE-striking Normandy–Vogelsberg Anticline and the NW-striking region of thick crust below the Ardennes and the Artois (Fig. 9). Thus, we suggest that the crustal dome below the Rhenish Massif is primarily due to interference between a linear lithospheric anticline and the shoulders of two linear grabens (Upper and Lower Rhine Grabens), rather than the consequence of an asthenospheric thermal anomaly. The magmatic activity, the thinned lithosphere and the seismic velocity anomaly in the asthenosphere can also be interpreted as due to interference between (1) a NNE-striking linear anomaly related to passive uplift of the asthenosphere below the Upper Rhine Graben, (2) a NW-striking linear anomaly related to passive uplift of the asthenosphere below the Lower Rhine Graben and (3) a NE-striking linear anomaly related to passive uplift of the asthenosphere below the Normandy–Vogelsberg Anticline.

Timing

Cenozoic sediments have been preserved in the Upper Rhine Graben, which intersects the lithospheric folds (Fig. 6). Hence, the respective timing of rifting and folding can be constrained by comparing the history of Cenozoic subsidence at several locations distributed along the strike of this graben. We use the Stafelfelden borehole, which is located in its southern part (i.e. on the hinge line of the Burgundy—Swabian Jura Anticline, Figs. 6, 8, 9), and the Sandhausen 4 and Spock 2 boreholes, which are located in its northern part (i.e. on the hinge line of the Sologne–Franconian Basin Syncline, Figs. 6, 8, 9). Both stations are located in areas where the amount of rift-related subsidence is greatest (Fig. 8).

Data and processing

The Cenozoic sedimentary sequence of the Upper Rhine Graben starts with thin (0–100 m) continental formations, which were unconformably deposited during the Eocene over the Paleozoic basement and the truncated Mesozoic

cover. Above Eocene continental deposits, the bulk of the sedimentary sequence is composed of shallow-marine, brackish to lacustrine sediments, 37–18 Ma in age. Sediments younger than 18 Ma are mostly continental (Sissingh 1998; Berger et al. 2005a, b).

Accumulation curves[1] were drawn, with the assumption that shallow-marine, brackish and lacustrine sediments were deposited at sea-level, whereas continental and fluviatile sediments were deposited between sea-level and the present-day elevation of the topographic surface (Fig. 12a, b). We relied on sedimentary environments and ages given by Berger et al. (2005a, b) and Derer et al. (2005) and on the curve of global sea-level computed by Abreu and Anderson (1998).

Long-wavelength deformation before rifting

The unconformity below Eocene continental deposits (Fig. 12a, b), which is known from southern France to the North Sea, indicates that a first event of long-wavelength deformation occurred prior to rifting. This event probably dates back to Late Cretaceous and Paleocene times, when wide parts of the European plate (including Provence, the Massif Central, the Bresse, the Jura, the Upper Rhine Graben, the Bohemian Massif, the Rhenish Massif and the Armorican Massif) rose above sea-level and were covered by continental alterites and lacustrine deposit. At the same time, the rate of subsidence increased in the Paris Basin, in the lower Rhône Valley and in the North Sea; intraplate deformation responsible for these vertical motions include basin inversion, upthrusting of basement blocks and lithospheric folding (Ziegler 1990; Ziegler et al. 1995; Guillocheau et al. 2000; Dèzes et al. 2004).

Cenozoic rifting and folding

In the northern part of the Upper Rhine Graben (Sandhausen 4 and Spock 2 boreholes, Fig. 12a), the main phase of accumulation started at 37 Ma and ended around 17 Ma. During this time interval, the amount of accumulation was 3,050 m, which is very close to the value of rifting-related subsidence computed from the geometry of the basement (3,000 m, Fig. 7). This suggests (1) that the sedimentary sequence related to rifting has been fully preserved in the northern part of the Upper Rhine Graben and (2) that the rifting event started at 37 Ma and ended at 17 Ma. This phase of rapid accumulation (0.15 mm/year on average) related to rifting was followed by a phase of slower accumulation (0.03 mm/year on average) between 17 and 0 Ma. The amount of accumulation during this second phase, which accelerated during the last 2 My, is 450 m in the northern part of the Upper Rhine Graben (Fig. 12a). This second accumulation phase cannot be attributed to rifting, because the full amount of rifting-related subsidence had been achieved between 37 and 17 Ma.

The geometry of top-basement (Fig. 7) demonstrates that subsidence related to rifting is equal in the northern and southern parts of the Upper Rhine Graben. If the timing of rifting is assumed to be the same also, then 3,050 m of rifting-related accumulation are to be expected between 37 and 17 Ma, in the southern part of the graben (Fig 11b). Now, in the Stafelfelden borehole, the preserved Cenozoic sedimentary sequence was deposited between 37 and 28.5 Ma; it is 2,050 m thick only. Therefore, it can be surmised that *ca.* 1,000 m of sediments were deposited during rifting, between 28.5 and 17 Ma, and have later been removed by erosion. 1,000 m of post-rift uplift of the southern part of the graben are required, to explain the present-day elevation of sedimentary horizons in the Stafelfelden borehole (Fig. 12b). This is consistent with the suggestion of Roll (1979) and Dèzes et al. (2004) that 1,000–1,500 m of syn-rift sediments have been eroded in the southern part of the Upper Rhine Graben.

Adding the amount of subsidence measured in the northern part of the Upper Rhine Graben (450 m) to the amount of uplift required in its southern part (1,000 m) gives 1,450 m of differential motion since 17 Ma. This value is very close to the amplitude of lithospheric folds inferred from the geometry of the basement (1,500 m, Fig. 9). Therefore, we attribute the 450 m accumulation in the northern part of the Upper Rhine Graben to subsidence of the Sologne–Franconian Basin Syncline and the 1,000 m uplift of its southern part to the rising of the Burgundy–Swabian Jura Anticline.

As a conclusion, the sedimentary record of the Upper Rhine Graben demonstrates that a first event of long-wavelength deformation affected the European plate before the onset of Cenozoic rifting (Fig. 13b). This event was responsible for the development of an unconformity below the syn-rift sedimentary infill. In the Upper Rhine Graben, rifting started at 37 Ma and the main phase of lithospheric stretching came to an end at about 17 Ma (Fig. 13c). Rifting in the southern segments of the ECRIS ended at the same time (Blès and Gros 1991; Séranne 1999; Michon and Merle 2001). After 17 Ma, lithospheric folding generated

[1] "Accumulation curves" show the thickness of compacted sediments accumulated in basins against time, whereas "subsidence curves" show vertical motions of the base of basins against time. Computing the history of subsidence from the history of accumulation requires paleobathymetry and variations of sea-level to be taken into account, and a decompaction procedure to be applied to the sedimentary sequence (Allen and Allen 1990). The decompaction procedure requires that porosity and compaction parameters are known for each stratigraphic interval. These parameters are not known in the boreholes described here. Thus, we did not decompact the sediments. The curves shown in this article are accumulation curves corrected for paleobathymetry and variations of sea-level.

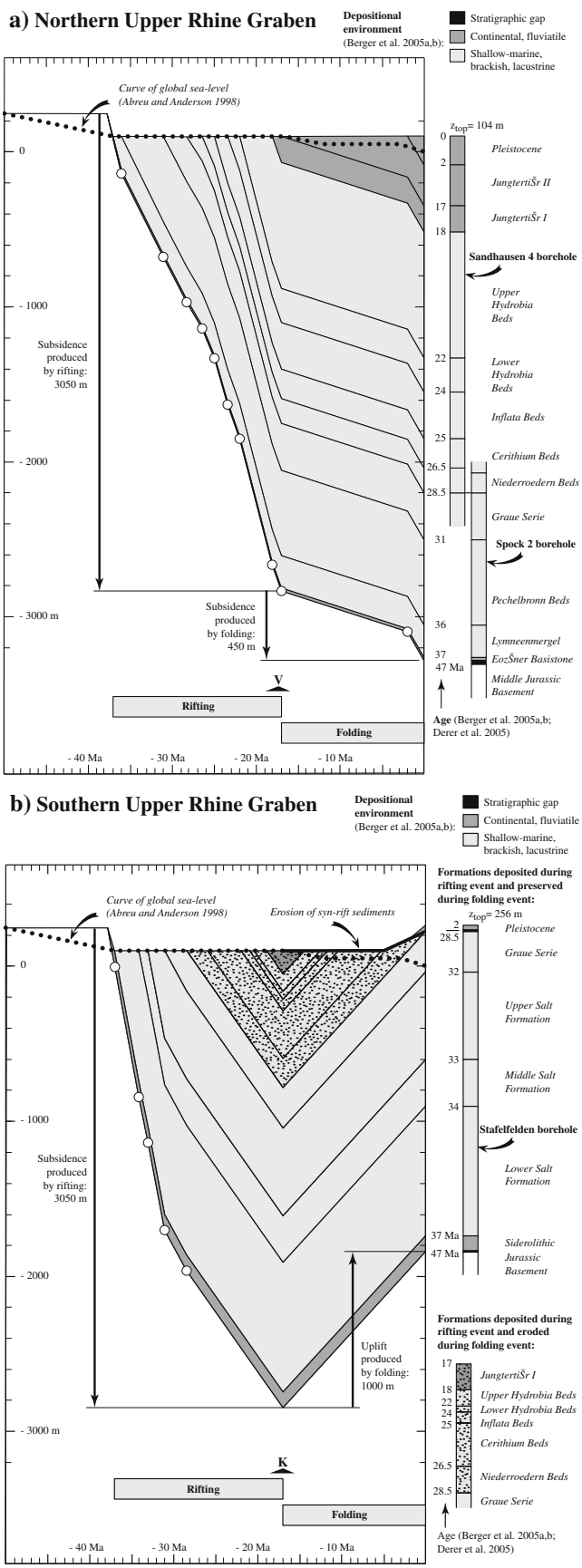

◀ **Fig. 12** Accumulation curves computed for **a** the northern part and **b** the southern part of the Upper Rhine Graben. Timing of volcanic activity (*K* Kaiserstuhl, *V* Vogelsberg) after Sissingh (2003) and Berger et al. (2005a, b)

continued subsidence of the northern part of the Upper Rhine Graben, while its southern part and the Rhenish Massif were uplifted (Fig. 13d). The transition from rifting to lithospheric folding at 17 Ma is consistent with the existence of an unconformity dated as mid-Burdigalian in the Upper Rhine, Bresse and Massif Central Grabens (Dèzes et al. 2004). It is consistent also with the development of a syn- to post-Burdigalian NE-striking synform in Sologne (Guillocheau et al. 2000).

Some faults affected the post-Burdigalian infill of the Upper Rhine Graben (Derer et al. 2005; Haimberger et al. 2005). The end of rift-related rapid accumulation at 17 Ma suggests that the post-Burdigalian activity of these faults was due mostly to local block adjustments during the development of the lithospheric folds, rather than to persistent lithospheric stretching.

Volcanic activity

Scattered volcanic activity occurred from the Paleocene to the Late Eocene in the Rhenish Massif, in the Vosges–Black Forest area, in the Massif Central and in the Bohemian Massif (Fig. 1). This early and moderate activity has been variously attributed to rifting, to lithospheric folding or to mantle plumes (Michon and Merle 2001; Dèzes et al. 2004; Michon and Merle 2005). The major phase of volcanism in the Rhenish Massif, in the Vosges–Black Forest area and in the Massif Central started only later during the Burdigalian, however, with the emplacement between *ca.* 20 and *ca.* 15 Ma, of the Kaiserstuhl, Vogelsberg, Siebengebirge and Westerwald volcanoes and with activity persisting until the Holocene in the Massif Central, in the Rhenish Massif (Eifel) and in the Swabian Jura (Höwenegg) (Michon and Merle 2001; Sissingh 2003; Dèzes et al. 2004; Berger et al. 2005a, b). The most productive regions (Vogelsberg, Eifel, Kaiserstuhl and Massif Central) are located at intersections of lithospheric anticlines with grabens; less productive regions (e.g. Swabian Jura) are located along hinge lines of lithospheric anticlines (Fig. 1). The major phase of volcanic activity started with the onset of lithospheric folding (Fig. 12). Therefore, Burdigalian volcanic activity may be attributed to the development of lithospheric anticlines; this activity was most intense in zones that had been thinned previously or were still thinning by rifting. Volcanic activity continued until the present day along hinge lines of lithospheric anticlines, preferentially at intersections with grabens (Eifel, Massif Central), but also in other areas (Swabian Jura).

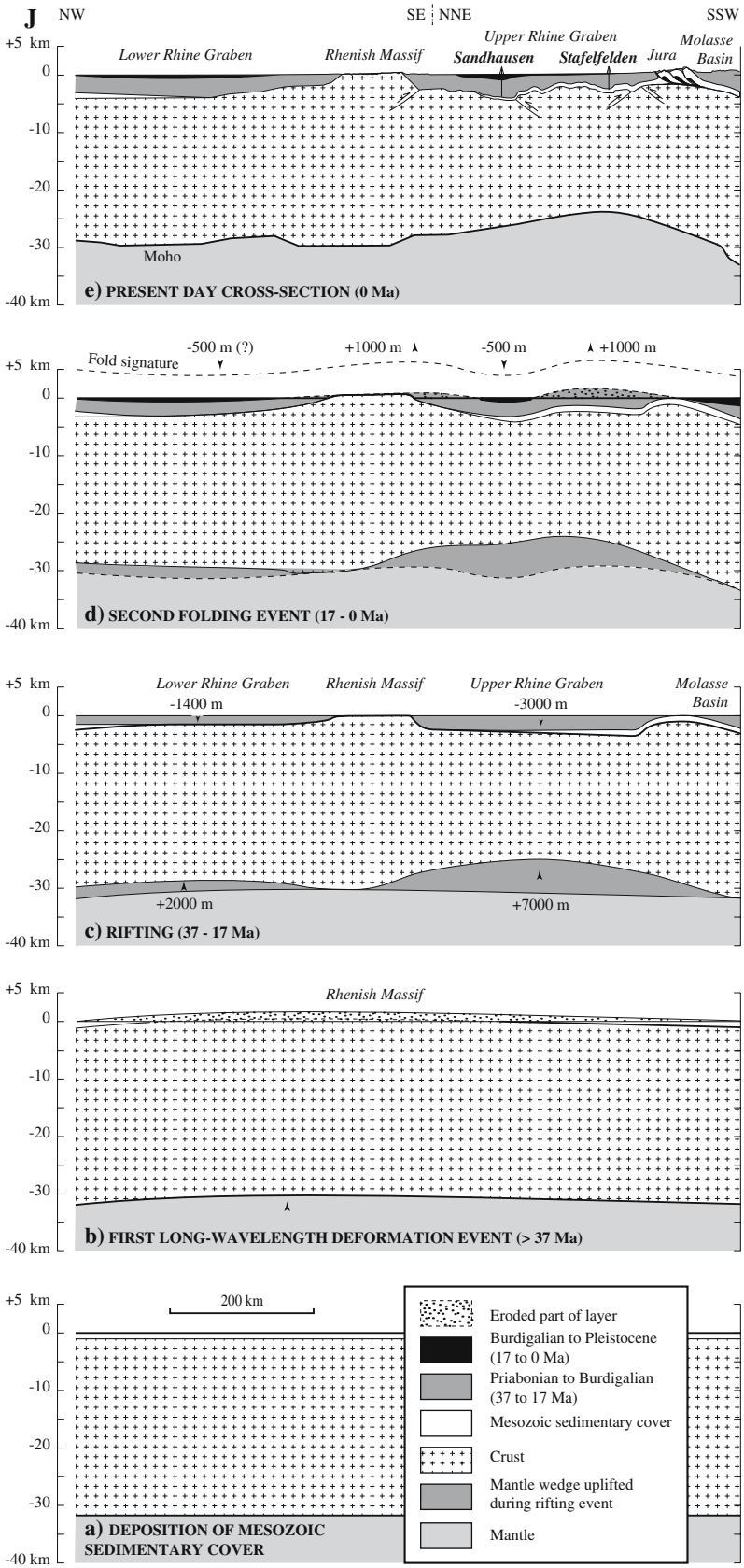

Fig. 13 Conceptual cross-sections, along the strike of the Upper and Lower Rhine Grabens (locations on Figs. 5, 6), illustrating how the present-day geometry of top-basement and Moho has resulted from superimposition of rifting and lithospheric folding. **a** Uniform Mesozoic sedimentary cover, 1,000 m thick, lies on basement; **b** before 37 Ma, a long-wavelength deformation event produces the base-Eocene unconformity; **c** between 37 and 17 Ma, rifting produces crustal thinning in the Upper and Lower Rhine Grabens, while foreland flexural bending produces subsidence in the Molasse Basin; **d** between 17 and 0 Ma, lithospheric folding produces crustal uplift on anticlines (southern Upper Rhine Graben and Rhenish Massif) and crustal subsidence in synclines (northern Upper Rhine Graben and Lower Rhine Graben); **e** actual geometry of top-basement and of Moho (computed from Figs. 5, 6) for comparison with (**d**). Lithospheric folding may have been accompanied (or replaced) by upper crustal thrusting during the Plio-Pleistocene

History of intraplate deformation in relation to the Alpine orogeny

Left-lateral transtension in ECRIS due to north-directed impingement of Adria into Europe (37–17 Ma)

The orientation of stresses during the development of the ECRIS is still debated (Bergerat 1987; Michon 2000; Merle and Michon 2001; Michon et al. 2003; Dèzes et al. 2004, 2005; Michon and Merle 2005; Ziegler and Dèzes 2005). Nevertheless, the geometry of the grabens in map view suggests that the ECRIS is primarily transtensional in origin: all the grabens, except the Lower Rhine Graben, are composed of lozenge-shaped segments separated from each other by NE-striking transfer faults (Fig. 1; Chorowicz and Deffontaines 1993; Schumacher 2002; Michon et al. 2003; Derer et al. 2005). The Valencia, Gulf of Lion, Lower Rhône, Valence, Bresse and Upper Rhine Grabens developed by a mixture of pure extensional and left-lateral strike-slip motions along their NNE-striking border faults. Pure left-lateral strike-slip motions occurred along the associated NE-striking transfer faults (Bergerat 1977a, b; Coulon 1992; Schumacher 2002; Behrmann et al. 2003; Michon et al. 2003; Dèzes et al. 2004, 2005; Derer et al. 2005; Lacombe and Jolivet 2005; Michon and Merle 2005; Schwarz and Henk 2005). Thus, as previously stated by Caire (1977) and Chorowicz and Deffontaines (1993), the ECRIS is primarily a left-lateral wrench zone, that strikes NE from the Mediterranean Sea to the Bohemian Massif (Fig. 3c–e).

Late Eocene initiation of this left-lateral wrench zone across the western European plate is consistent with events that occurred simultaneously at the southern margin of western Europe. From the Late Cretaceous to the Eocene, this margin was dominated by subduction of the Ligurian Ocean below Europe and of the Valaisan Ocean below Adria (Fig. 3a, b). By Late Eocene, the Valais Ocean was closed. Crustal shortening of the European margin under the north-directed impingement of Adria started while the subduction of the Ligurian Ocean was still ongoing west of Adria (Fig. 3c) (Dèzes et al. 2004; Lacombe and Jolivet 2005). Therefore, the formation of the ECRIS can be attributed to the development of a left-lateral wrench zone separating the foreland of the Adriatic collision zone from the foreland of the Corsica–Sardinia–Rif subduction belt. Impingement of Adria into Europe, after the closure of the Valais Ocean, was responsible for development of this wrench zone (Fig. 3c, d, e).

Lithospheric folding due to NW-directed shortening between Adria and Europe (17–0 Ma)

The transition from rifting to intraplate folding during the Burdigalian is consistent with events that occurred simultaneously at the southern border of the European plate. Back-arc oceanic spreading started at 21.5 Ma at the emplacement of the Gulf of Lion and led to the development of the Provençal Basin (Fig. 3e) (Dèzes et al. 2004). This was accompanied by southeastwards retreat and counter-clockwise rotation of the Corsica–Sardinia subduction belt (Rosenbaum and Lister 2004; Lacombe and Jolivet 2005). Paleomagnetic data (Dewey et al. 1989; Rosenbaum et al. 2002) as well as stretching lineations in the Alps (Choukroune et al. 1986; Schmid and Kissling 2000) indicate a change in the direction of motion of Adria during the Cenozoic, from north-south to NW–SE. This change has been dated at 9 Ma by Dewey et al. (1989). However, new paleogeographic reconstructions based on a re-interpretation of paleomagnetic data indicate that this change occurred at about 20 Ma (Rosenbaum et al. 2002). The opening of the Provençal Basin at 21.5 Ma and the history of intraplate deformation in the NW-Alpine foreland are consistent with these new reconstructions. Rifting in the southern part of ECRIS (Lower Rhône Valley, Bresse and Massif Central) came to an end between 21.5 and 17 Ma (Blès and Gros 1991; Séranne 1999; Michon and Merle 2001). We have demonstrated that a transition from rifting to lithospheric folding occurred at 17 Ma in the region of the Upper Rhine Graben. On the basis of the chronological coincidence between all these events, we attribute the end of rifting and the onset of lithospheric folding to the change in azimuth of convergence between Adria and Europe, in connection with the opening of the oceanic Provençal Basin (Fig. 3f, g). Persistence until the present-day of NE-directed lithospheric stretching in the Lower Rhine Graben (Dèzes et al. 2004) is consistent with the development of lithospheric folds under NW-directed lithospheric shortening (Fig. 3f, g, h).

Several authors have suggested that pre-existing basement faults striking NE have been reactivated in transpression recently in the Rhenish Massif (Ahorner 1975, 1983; Anderle 1987; Schwab 1987; Hinzen 2003; Schäfer et al. 2005), at the northern front of the Jura fold-and-thrust belt (Laubscher 1998; Giamboni et al. 2004) and south of the Vosges (Rotstein et al. 2005). In addition, the cross-sectional distribution of earthquakes below the Vosges and Black Forest suggests that the Burgundy–Swabian Jura Anticline is currently evolving into a tectonic wedge, which starts to thrust northwards over the Sologne–Franconian Basin Syncline (Édel et al. 2007). This possibly indicates a transition from lithospheric folding to upper crustal thrusting during the Plio-Pleistocene (Fig. 13e). Such a transition would provide an explanation (1) for the recent acceleration of subsidence in the northern part of the Upper Rhine Graben and in the Lower Rhine Graben (Figs. 10a and c; Zijerveld et al. 1992; Geluk et al. 1994; Michon et al. 2003; Schäfer et al. 2005) and (2) for the recent acceleration of uplift in the Rhenish Massif

(Fig. 10c; Garcia-Castellanos et al. 2000; Meyer and Stets 2002; Schäfer et al. 2005).

Conclusions

The present-day crustal geometry of the NW-Alpine foreland includes interfering signatures of lithospheric thinning in the ECRIS and lithospheric folding. Both features represent intraplate deformation produced by the Alpine orogeny. We have separated their geometrical and chronological signatures.

The ECRIS is primarily a left-lateral wrench zone that strikes NE from the Mediterranean Sea to the Bohemian Massif. It is composed of left-lateral strike-slip faults striking NE, of left-lateral transtensional grabens striking NNE and of a purely extensional graben striking NW (the Lower Rhine Graben). This wrench zone developed mostly from 37 to 17 Ma; it acted as a transfer zone separating the foreland of the Adriatic collision zone from the foreland of the Corsica–Sardinia–Rif subduction belt.

Lithospheric folds striking NE developed from 17 Ma to the present, in response to NW-directed shortening between Europe and Adria. The geometry of these folds (wavelength = 270 km; amplitude = 1,500 m) is consistent with the geometry, as predicted by analogue and numerical models, of buckle folds produced by horizontal shortening of the whole lithosphere. Lithospheric folding is responsible for the Burdigalian onset of volcanic activity; volcanism was most active where anticlines intersected areas that had been thinned previously (or were still thinning) by rifting. Scattered volcanic activity persists until the present day along the crest of some lithospheric anticlines.

Acknowledgements This work was performed partly in 2000–2002, while OB and MD held post-doctoral positions supervised by MF at the Centre de Recherches Pétrographiques et Géochimiques of Nancy (CNRS-UPR 2300). We acknowledge financial support from the Région Lorraine, from the Bureau de Recherches Géologiques et Minières (Geofrance 3D project) and from the CNRS-INSU (Programme National Intérieur de la Terre 2001–2002, Theme V "Rapid vertical motions"). Sandhausen 4 and Spock 2 borehole data (Fig. 12) were made available by the Landesamt fur Geologie, Rohstoffe und Bergbau of Baden-Württemberg. We thank our colleagues of the EUCOR-URGENT project for inviting us to their annual workshops. Our results and interpretations benefited from constructive discussions with Sierd Cloetingh, François Guillocheau, Laurent Michon, Cécile Robin and Stefan Schmid. We thank Pierre Dèzes, Peter Ziegler and an anonymous reviewer for their critical comments on the manuscript.

References

Abreu VS, Anderson JB (1998) Glacial eustasy during the Cenozoic: sequence stratigraphic implications. Am Assoc Petrol Geol Bull 82:1385–1400

Ahorner L (1975) Present-day stress field and seismotectonic block movements along major fault zones in Central Europe. Tectonophysics 29:233–249

Ahorner L (1983) Historical seismicity and present-day microearthquake activity of the Rhenish Massif, Central Europe. In: Fuchs K, von Gehlen K, Melzer M, Murawski H, Semmel A (eds) Plateau uplift, the Rhenish shield—a case history. Springer, Berlin, pp 198–221

Allen PA, Allen JR (1990) Basin analysis: principles and applications. Blackwell Science, Oxford, pp 1–451

Allen PA, Homewood P, Williams GD (1986) Foreland basins: an introduction. Foreland basins symposium. Spec Publ Int Assoc Sedimentol 8:3–12

Anderle HJ (1987) The evolution of the South Hunsrück and Taunus Borderzone. Tectonophysics 137:101–114

Babushka V, Plomerova J (1992) The lithosphere in Central Europe—seismological and petrological approach. Tectonophysics 207:141–163

Barbarand J, Lucazeau F, Pagel M, Séranne M (2001) Burial and exhumation history of the south-eastern Massif Central (France) constrained by apatite fission-track thermochronology. Tectonophysics 335:275–290

Beaumont C (1979) On rheological zonation of the lithosphere during flexure. Tectonophysics 59:347–365

Becker A (2000) The Jura Mountains—an active foreland fold-and-thrust belt? Tectonophysics 321:381–406

Behrmann JH, Hermann O, Horstmann M, Tanner DC, Bertrand G (2003) Anatomy and kinematics of oblique continental rifting revealed: a three-dimensional case study of the southeast Upper Rhine graben (Germany). Am Assoc Petrol Geol Bull 87:1105–1121

Berger JP, Reichenbacher B, Becker D, Grimm M, Grimm K, Picot L, Storni A, Pirkenseer C, Derer C, Schaefer A (2005a) Paleogeography of the Upper Rhine Graben (URG) and the Swiss Molasse Basin (SMB) from Eocene to Pliocene. Int J Earth Sci 94:697–710

Berger JP, Reichenbacher B, Becker D, Grimm M, Grimm K, Picot L, Storni A, Pirkenseer C, Schaefer A (2005b) Eocene-Pliocene time scale and stratigraphy of the Upper Rhine Graben (URG) and the Swiss Molasse Basin (SMB). Int J Earth Sci 94:711–731

Bergerat F (1977a) Le rôle des décrochements dans les liaisons tectoniques entre le Fossé de la Saône et le Fossé Rhénan. C R Somm Soc Géol Fr 4:195–199

Bergerat F (1977b) La fracturation dans l'avant-pays jurassien entre les fossés de la Saône et du Rhin. Analyse et essai d'interprétation dynamique. Rev Géogr Phys Géol Dyn 19:325–338

Bergerat F (1987) Stress fields in the European platform at the time of Africa-Eurasia collision. Tectonics 6:99–132

Bergerat F, Geyssant J (1980) La fracturation tertiaire de l'Europe du Nord: résultat de la collision Afrique-Europe. C R Acad Sci Paris Sér D 390:1521–1524

Bergerat F, Mugnier JL, Guellec S, Trufferrt C, Cazes M, Damotte B, Roure F (1990) Extensional tectonics and subsidence of the Bresse basin: an interpretation from ECORS data. Mém Soc Géol Fr 156:145–156

Blès JL, Gros Y (1991) Stress field changes in the Rhone Valley from the Miocene to the present. Tectonophysics 194:265–277

Bourgeois O, Le Carlier de Veslud C, Ford M, Diraison M (2001) Propagation of the Alpine forebulge into the southern Upper Rhine Graben? In: Abstract of the 2nd EUCOR-URGENT Workshop, vol 8. Mont Saint-Odile, Strasbourg (France), 7–11 October 2001

Bourgeois O, Ford M, Pik R, Le Carlier de Veslud C, Gerbault M, Diraison M, Ruby N, Bonnet S (2004) Vertical motions around the Rhine Graben: separation of rifting and lithospheric folding signatures. In: proceedings of the RST-GV international joint meeting, Strabourg (France), Abst. Number: RSTGV-A-00294

Brun JP (1999) Narrow rifts versus wide rifts: inferences for the mechanics of rifting from laboratory experiments. Philos Trans R Soc Lond A 357:695–712

Brun JP, Gutscher MA, DEKORP-ECORS team (1992) Deep crustal structure of the Rhine Graben from DEKORP-ECORS seismic reflection data. Tectonophysics 208:39–147

Buck RW (1991) Modes of continental lithospheric extension. J Geophys Res 96:20161–20178

Bull JM, Martinod J, Davy P (1992) Buckling of the oceanic lithosphere from geophysical data and experiments. Tectonics 11:537–548

Burg JP, Van Den Driessche J, Brun JP (1994a) Syn- to post-thickening extension in the Variscan Belt of Western Europe: modes and structural consequences. Géol Fr 3:33–51

Burg JP, Van Den Driessche J, Brun JP (1994b) Syn- to post-thickening extension: mode and consequences. C R Acad Sci II: Sciences de la Terre et des Planètes 319:1019–1032

Burkhard M, Sommaruga A (1998) Evolution of the Western Swiss Molasse basin: structural relations with the Alps and the Jura belt. In: Mascles A, Puigdefàbregas C, Luterbacher HP, Fernàndez M (eds) Cenozoic foreland basins of Western Europe. Geol Soc (Lond) Spec Publ 134:279–298

Burov EB, Lobkovsky LI, Cloetingh S, Nikishin AM (1993) Continental lithosphere folding in Central Asia (Part II): constraints from gravity and topography. Tectonophysics 226:73–87

Caire A (1977) Interpretation unitaire des fosses des Limagnes, de la Bresse et du Rhin. C R Acad Sci Paris 285:1279–1281

Chantraine J, Autran A, Cavelier A, et al (1996) Carte Géologique de la France à 1/000 000, 6th edn. Bur Rech Geol Min, Orléans (France)

Chase CG, Libarkin JA, Sussman AJ (2002) Colorado plateau: geoid and means of isostatic support. Int Geol Rev 44:575–587

Chorowicz J, Deffontaines B (1993) Transfer faults and pull-apart model in the Rhine graben from analysis of multisource data. J Geophys Res 98:14339–14351

Choukroune P, Ballèvre M, Cobbold PR, Gautier Y, Merle O, Vuichard JP (1986) Deformation and motion in the western Alpine Arc. Tectonics 5:215–226

Cloetingh S, Burov E, Poliakov A (1999) Lithosphere folding: primary response to compression? (from central Asia to Paris basin). Tectonics 18:1064–1083

Coulon M (1992) La distension oligocène dans le nord-est du bassin de Paris (perturbation des directions d'extension et distribution des stylolites). Bull Soc Géol Fr 163:531–540

Cox KG (1989) The role of mantle plumes in the development of continental drainage patterns. Nature 342:873–877

Cox KG (1993) Continental magmatic underplating. Philos Trans R Soc Lond A 342:155–166

Debrand-Passard S (ed) (1984) Synthèse Géologique du Sud-Est de la France, Mém BRGM 125:1–615, Bur Rech Géol Min, Orléans

Derer CE, Schumacher ME, Schäfer A (2005) The northern Upper Rhine Graben: basin geometry and early syn-rift tectono-sedimentary evolution. Int J Earth Sci 94:640—656

Dewey JF, Windley BF (1988) Palaeocene-Oligocene tectonics of NW Europe. In: Morton AC, Parson LM (eds) Early tertiary volcanism and the opening of the NE Atlantic. Geol Soc (Lond) Spec Publ 39:25–31

Dewey JF, Helman ML, Turco E, Hutton DHW, Knott SD (1989) Kinematics of the western Mediterranean. In: Coward MP, Dietrich D, Park RG (eds) Alpine tectonics. Geol Soc (Lond) Spec Publ 45:65–283

Dèzes P, Schmid SM, Ziegler PA (2004) Evolution of the european cenozoic rift system; interaction of the Pyrenean and Alpine orogens with the foreland lithosphere. Tectonophysics 389:1–33

Dèzes P, Schmid SM, Ziegler PA (2005) Reply to comments by L. Michon and O. Merle on "Evolution of the European Cenozoic Rift System; interaction of the Pyrenean and Alpine orogens with the foreland lithosphere" by P. Dèzes, S. M. Schmid and P. A. Ziegler. Tectonophysics 401:257–262

Édel JB, Whitechurch H, Diraison M (2007) Seismicity wedge beneath the Upper Rhine Graben due to backwards alpine push? Tectonophysics 428:49–64

Ford M, Lickorish WH (2004) Foreland basin evolution around the western Alpine arc. In: Joseph P, Lomas S (eds) New perspectives on Turbidites, the Grès d'Annot Sandstones, SE France. Geol Soc (Lond) Spec Publ 221:39–63

Ford M, Duchêne S, Gasquet D, Vanderhaeghe O (2006) Two-phase orogenic convergence in the external and internal SW Alps. J Geol Soc (Lond) 163:815–826

Gapais D, Cobbold PR, Bourgeois O, Rouby D, de Urreiztieta M (2000) Tectonic significance of fault-slip data. J Struct Geol 22:881–888

Garcia-Castellanos D, Cloetingh S, van Balen R (2000) Modelling the middle Pleistocene uplift in the Ardennes-Rhenish Massif: thermo-mechanical weakening under the Eifel. Global Planet Changes 27:39–52

Geluk MC, Duin EJT, Dusar M, Rijkers RHB, van den Berg MW, van Rooijen P (1994) Stratigraphy and tectonics of the Roer Valley Graben. Geol Mijnb 73:129–141

Gerbault M (2000) At what stress level is the central Indian Ocean lithosphere buckling? Earth Planet Sci Lett 178:165–181

Gerbault M, Burov EB, Poliakov ANB, Daignieres M (1999) Do faults trigger folding in the lithosphere? Geophys Res Lett 26:271–274

Giamboni M, Wetzel A, Nivière B, Schumacher M (2004) Plio-Pleistocene folding in the southern Rhinegraben recorded by the evolution of the drainage network (Sundgau area; northwestern Swizerland and France). Eclogae Geol Helv 97:17–31

Guillocheau F, Robin C, Allemand P, Bourquin S, Brault N, Dromart G, Friedenberg Garcia JP, Gaulier JM, Gaumet F, Grosdoy B, Hanot F, Le Strat P, Mettraux M, Nalpas T, Prijac C, Rigollet C, Serrano O, Grandjean G (2000) Meso-cenozoic geodynamic evolution of the Paris basin: 3D stratigraphic constraints. Geodin Acta 13:189–245

Gutscher MA (1995) Crustal structure and dynamics in the Rhine Graben and the Alpine foreland, Geophys J Int 122:617–636

Haimberger R, Hoppe A, Schäfer A (2005) High-resolution seismic survey on the Rhine River in the northern Upper Rhine Graben. Int J Earth Sci 94:657–668

Hinzen KG (2003) Stress field in the Northern Rhine area, Central Europe, from earthquake fault plane solutions. Tectonophysics 377:325–356

Jones SM, White N, Clarke BJ, Rowley E, Gallagher K (2002) Present and past influence of the Iceland plume on sedimentation. Geol Soc (Lond) Spec Publ 196:13–25

Jowett EC (1991) Post-collisional formation of the Alpine foreland rifts. Ann Soc Geol Pol 61:37–59

Karg H, Carter A, Brix MR, Littke R (2005) Late- and post-Variscan cooling and exhumation history of the northern Rhenish massif and the southern Ruhr Basin: new constraints from fission-track analyses. Int J Earth Sci 94:180–192

Keyser M, Ritter JRR, Jordan M (2002) 3D shear-wave velocity structure of the Eifel plume, Germany. Earth Planet Sci Lett 203:59–82

Kooi H, Cloetingh S (1992) Lithospheric necking and regional isostasy at extensional basins. J Geophys Res 97:17553–17591

Kusznir NJ, Ziegler PA (1992) The mechanics of continental extension and sedimentary basin formation: a simple-shear/pure-shear flexural cantilever model. Tectonophysics 215:117–131

Lacombe O, Jolivet L (2005) Structural and kinematic relationships between Corsica and the Pyrenees-Provence domain at the time of the Pyrenean orogeny. Tectonics 24:1–20

Laubscher HP (1986) The eastern Jura: relations between thinskinned and basement tectonics, local and regional. Geol Rundsch 75:535–553

Laubscher HP (1992) Jura kinematics and the Molasse Basin. Eclogae Geol Helv 85:653–675

Laubscher HP (1998) The complex encounter of Rhine graben and Jura at the eastern margin of the Laufen Basin. Eclogae Geol Helv 91:275–291

Lefort JP, Agarwal BNP (1996) Gravity evidence for an Alpine buckling of the crust beneath the Paris Basin. Tectonophysics 258:1–14

Lefort JP, Agarwal BNP (2002) Topography of the Moho undulations in France from gravity data: their age and origin. Tectonophysics 350:193–213

Leseur N, Mollier M, Ford M, Bourlange S, Bourgeois O (2005) Three dimensional flexure of the European plate north of the Alps. In: proceedings of the SGF-SGE joint earth science meeting on thrust belts and foreland basins, Rueil-Malmaison (France), 14–16 December 2005

Link K, Rahn M, Keller J, Stuart F, Diskin S (2003) Thermo-tectonic evolution of the Upper Rhine Graben rift flanks constrained by FT and (U-Th/He) analyses. In: Abstract of the 4th EUCOR-URGENT Workshop, vol 35. Basel (Switzerland), 29 September–1 October 2003

Lithgow-Bertelloni C, Silver PG (1998) Dynamic topography, plate driving forces and the African superswell. Nature 395:269–272

Martinod J, Davy P (1992) Periodic instabilities during compression of the lithosphere 1. Deformation modes from an analytical perturbation method. J Geophys Res 92:1999–2014

Martinod J, Davy P (1994) Periodic instabilities during compression of the lithosphere 2. Analogue experiments. J Geophys Res 99:12057–12069

Martinod J, Molnar P (1995) Lithospheric folding in the Indian Ocean and the rheology of the oceanic plate. Bull Soc Géol Fr 166:813–821

McKenzie D (1978) Some remarks on the development of sedimentary basins. Earth Planet Sci Lett 40:25–32

McKenzie (1984) The generation and compaction of partially molten rock. J Petrol 25:713–765

Mégnien C (ed) (1980) Synthése Géologique du Bassin de Paris I, II and III. Mém BRGM 102–103:1–467, Bur Rech Géol Min, Orléans

Merle O, Michon L (2001) The formation of the West European rift: a new model as exemplified by the Massif Central area. Bull Soc Géol Fr 172:213–221

Merle O, Michon L, Camus G, De Goer A (1998) Oligocene extensional processes along the northern transect of the Massif central rift (France). Bull Soc Géol Fr 169:615–626

Meyer W, Stets J (2002) Pleistocene to recent tectonics in the Rhenish Massif (Germany). Neth J Geosci 81:217–221

Michon L (2000) Dynamique de l'Extension Continentale—Application au Rift Ouest-Européen par l'Étude de la Province du Massif Central. Unpublished Ph.D. Thesis, Université Blaise Pascal, Clermont-Ferrand (France)

Michon L, Merle O (2001) The evolution of the Massif Central rift: spatio-temporal distribution of the volcanism. Bull Soc Géol Fr 172:201–211

Michon L, Merle O (2005) Discussion on "Evolution of the European Cenozoic Rift System: interaction of the Alpine and Pyrenean orogens with their foreland lithosphere" by P. Dèzes, S. M. Schmid and P. A. Ziegler. Tectonophysics 401:251–256

Michon L, van Balen RT, Merle O, Pagnier H (2003) The cenozoic evolution of the Roer Valley rift system integrated at a European scale. Tectonophysics 367:101–126

Munck F, Sauer K (eds) (1979) Synthése Géothermique du Fossé Rhénan Supérieur. Bur Rech Geol Min Alsace/Geol Landesamt Baden-Wurttemberg. Strasbourg (France)/Freiburg (Germany)

Neugebauer HJ (1978) Crustal doming and mechanisms of rifting: part 1. Rift formation. Tectonophysics 45:159–186

Peyaud JB, Barbarand J, Carter A, Pagel M (2005) Mid-cretaceous uplift and erosion on the northern margin of the Ligurian Tethys deduced from thermal history reconstruction. Int J Earth Sci 94:462–474

Philippe Y, Colletta B, Mascle E (1996) The Jura fold-and-thrust belt: a kinematic model based on map-balancing. In: Ziegler PA, Horvath F (eds) Structure and prospects of Alpine basins and forelands. Peri-Tethys Mem 2, Mém Mus Natl Hist Nat Paris 170:235–261

Prodehl C, Mueller S, Glahn A, Gutscher M, Haak V (1992) Lithospheric cross sections of the European cenozoic rift system. Tectonophysics 208:113–138

Regenauer-Lieb K, Petit JP (1997) Cutting of the European continental lithosphere: plasticity theory applied to the present Alpine collision. J Geophys Res 102:7731–7746

Ritter JRR, Jordan M, Christensen UR, Achauer U (2001) A mantle plume below the Eifel volcanic fields, Germany. Earth Planet Sci Lett 186:7–14

Roll A (1979) Versuch einer Volumenbilanz des Oberrheingrabens und seiner Schultern. Geol Jahrb A52:1–82

Rosenbaum G, Lister GS (2004) Neogene and quaternary rollback evolution of the Tyrrhenian Sea, the Apennines, and the Sicilian Maghrebides. Tectonics 23:TC1013

Rosenbaum G, Lister GS, Duboz C (2002) Relative motion of Africa, Iberia and Europe during Alpine orogeny. Tectonophysics 359:117–129

Rotstein Y, Schaming M, Rousse S (2005) Tertiary tectonics of the Dannemarie basin, Upper Rhine Graben, and regional implications. Int J Earth Sci 94:669–679

Rousset D, Bayer R, Guillon D, Edel JB (1993) Structure of the southern Rhine Graben from gravity and reflection seismic data (ECORS-DEKORP program). Tectonophysics 221:135–153

Schäfer A, Utescher T, Klett M, Valdivia-Manchego M (2005) The cenozoic Lower Rhine basin—rifting, sedimentation, and cyclic stratigraphy. Int J Earth Sci 94:621–639

Schettino A, Scotese C (2002) Global kinematic constraints to the tectonic history of the Mediterranean region and surrounding areas during the Jurassic and Cretaceous. In: Rosenbaum G, Lister GS (eds) Reconstruction of the evolution of the Alpine-Himalayan orogen. J Virtual Explor 8:145–160

Schmid SM, Kissling E (2000) The arc of the western Alps in the light of geophysical data on deep crustal structure. Tectonics 19:62–85

Schumacher ME (2002) Upper Rhine Graben: the role of preexisting structures during rift evolution. Tectonics 21:1–17. doi:10.1029/2001TC900022

Schwab K (1987) Compression and right-lateral strike-slip movement at the Southern Hunsrück Borderfault (Southwest Germany). Tectonophysics 137:115–122

Schwarz M, Henk A (2005) Evolution and structure of the Upper Rhine Graben: insights from three-dimensional thermomechanical modelling. Int J Earth Sci 94:732–750

Sengör AMC (1976) Collision of irregular continental margins: implications for foreland deformation of Alpine-type orogens. Geology 4:779–782

Sengör AMC, Burke K, Dewey JF (1978) Rifts at high angles to orogenic belts: tests for their origin and the Upper Rhine Graben as an example. Am J Sci 278:24–40

Séranne M (1999) The Gulf of Lion continental margin (NWMediterranean) revisited by IBS: an overview. In: Durand B, Jolivet L, Horvath F, Séranne M (eds) The Mediterranean Basins: tertiary extension within the Alpine orogen. Geol Soc (Lond) Spec Publ 156:15–36

Sinclair HD, Coakley BJ, Allen PA, Watts AB (1991) Simulation of foreland basin stratisgraphy using a diffusion model of mountain belt uplift and erosion: an example from the central Alps, Switzerland. Tectonics 10:599–620

Sissingh W (1998) Comparative tertiary stratigraphy of the Rhine Graben, Bresse Graben and Molasse basin: correlation of Alpine foreland events. Tectonophysics 300:249–284

Sissingh W (2003) Tertiary paleogeographic and tectonostratigraphic evolution of the rhenish triple junction. Palaeogeogr Palaeoclimatol Palaeoecol 196:229–263

Sommaruga A (1999) Decollement tectonics in the Jura foreland fold-and-thrust belt. Mar Petrol Geol 16:111–134

Stampfli GM, Mosar J, Marquer D, Marchant R, Baudin T, Borel G (1998) Subduction and obduction processes in the Alps. Tectonophysics 296:159–204

Stewart J, Watts AB (1997) Gravity anomalies and spatial variations of flexural rigidity at mountain ranges. J Geophys Res 102:5327–5352

Tapponnier P (1977) Évolution tectonique du système Alpin en Mediterranée: poinçonnement et écrasement rigide-plastique. Bull Soc Géol Fr Sér 7 19:437–460

Turcotte DL, Schubert G (2002) Geodynamics, 2nd edn. Cambridge University Press, Cambridge (UK), pp 1–528

Van Balen RT, Houtgast RF, Van der Wateren FM, Vandenberghe J (2002) Neotectonic evolution and sediment budget of the Meuse catchment in the Ardennes and the Roer Valley Rift System. In: Schäfer A, Siehl A (eds) Rift tectonics and syngenetic sedimentation—the Cenozoic Lower Rhine basin and related structures. Neth J Geosci Geol Mijnb 81:211–215

Watts AB (2001) Isostasy and flexure of the lithosphere. Cambridge University Press, Cambridge (UK), pp 1–480

Zeyen H, Novak O, Landes M, Prodehl C, Driard L, Hirn A (1997) Refraction-seismic investigations of the northern Massif Central (France). Tectonophysics 275:99–117

Ziegler PA (1988) Evolution of the Arctic-North Atlantic and the Western Tethys. Am Assoc Petrol Geol Mem 43:198

Ziegler PA (1990) Geological Atlas of Western and Central Europe, 2nd edn. Shell Internat Petrol Mij, distributed by Geol Soc Publ House, Bath, pp 1–239, 56 encl

Ziegler PA (1994) Cenozoic rift system of western and central Europe: an overview. Geol Mijnb 73:99–127

Ziegler PA, Cloetingh S, van Wees JD (1995) Dynamics of intra-plate compressional deformation: the Alpine foreland and other examples. Tectonophysics 252:7–59

Ziegler PA, Cloetingh S (2004) Dynamic processes controlling evolution of rifted basins. Earth Sci Rev 64:1–50

Ziegler PA, van Wees JD, Cloetingh S (1998) Mechanical controls on collision-related compressional intraplate deformation. Tectonophysics 300:103–129

Ziegler PA, Schumacher M, Dèzes P, van Wees JD, Cloetingh S (2004) Post-variscan evolution of the lithosphere in the Rhine Graben area: constraints from subsidence modelling. In: Wilson M, Neumann ER, Davies GR, Timmerman MJ, Heeremans M, Larsen BT (eds) Permo-carboniferous magmatism and rifting in Europe. Geol Soc (Lond) Spec Publ 222:289–317

Ziegler PA, Dèzes P (2005) Evolution of the lithosphere in the area of the Rhine Rift System. Int J Earth Sci 94:594–614

Zijerveld L, Stephenson R, Cloetingh S, Duin E, Van Den Berg MW (1992) Subsidence analysis and modelling of the Roer Valley Graben (SE Netherlands). Tectonophysics 208:159–171